

NASA TECHNICAL NOTE



NASA TN D-4838

C.1

NASA TN D-4838



LOAN COPY: RETURN TO
AFWL (WLIL-2)
KIRTLAND AFB, N MEX

THE EXCITATION SPECTRUM FOR A BOSE GAS WITH REPULSIVE AND ATTRACTIVE INTERACTIONS

by Gerald V. Brown
Lewis Research Center
Cleveland, Ohio

NATIONAL AERONAUTICS AND SPACE ADMINISTRATION • WASHINGTON, D. C. • OCTOBER 1968



THE EXCITATION SPECTRUM FOR A BOSE GAS WITH
REPULSIVE AND ATTRACTIVE INTERACTIONS

By Gerald V. Brown

Lewis Research Center
Cleveland, Ohio

NATIONAL AERONAUTICS AND SPACE ADMINISTRATION

For sale by the Clearinghouse for Federal Scientific and Technical Information
Springfield, Virginia 22151 - CFSTI price \$3.00

ABSTRACT

The correct qualitative features of the helium II elementary excitation spectrum are derived microscopically for a realistic interatomic potential. The strong repulsive core is included by using a reaction matrix in the Hamiltonian. The attractive well is successfully included by assuming a generalized Bose-Einstein condensation. The pair Hamiltonian is diagonalized by the thermodynamically equivalent Hamiltonian method. Numerical solutions yield spectra with phonon and roton regions. The spectrum energies are too high for the Yntema-Schneider potential. Another potential, constructed to fit virial coefficient data classically, gives better results. Spectra are presented for a series of attractive well strengths.

THE EXCITATION SPECTRUM FOR A BOSE GAS WITH REPULSIVE AND ATTRACTIVE INTERACTIONS

by Gerald V. Brown

Lewis Research Center

SUMMARY

The correct qualitative features of the helium II elementary excitation spectrum are derived microscopically for a realistic interatomic potential. The strong repulsive core is included by using a reaction matrix in the Hamiltonian. The attractive well is successfully included by assuming a generalized Bose-Einstein condensation. The pair Hamiltonian is diagonalized by the thermodynamically equivalent Hamiltonian method. Numerical solutions yield spectra with phonon and roton regions. The spectrum energies are too high for the Yntema-Schneider potential. Another potential, constructed to fit virial coefficient data classically, gives better results. Spectra are presented for a series of attractive well strengths.

INTRODUCTION

The attempts which have been made to explain the unusual properties of superfluid helium (He II) have met with success or with difficulties, depending on the level of the approach. On the successful side are the phenomenological theories with empirically adjusted parameters. On the less successful side are the microscopic theories which attempt to derive the properties of liquid helium II from the interatomic forces of helium atoms. No microscopic theory has been able to deduce the energy spectrum (energy as a function of momentum) for a realistic potential. Prior to the present work, not even the qualitative features of the spectrum (the phonon-like part and the roton minimum) have been successfully derived from an interatomic potential including both strong repulsion and an attractive well.

The phenomenological derivations of the spectrum are well known. Landau (refs. 1 and 2) deduced from specific heat data that the spectrum of elementary excitations in helium should contain a phonon-like part (a linear portion at and near zero momentum) and

a group of higher energy excitations, which he termed "rotons." The energies of these excitations were postulated (refs. 1 and 2) to be

$$\left. \begin{aligned} E_{\text{phonon}} &= cp \\ E_{\text{roton}} &= \frac{(p - p')^2}{2\mu} + \Delta \end{aligned} \right\} \quad (1)$$

where p is momentum and c , p' , μ , and Δ are constants adjusted to fit the experimental specific heat data. The phonon-like excitations contribute a T^3 term to the specific heat, whereas the roton excitations make an exponential contribution because of the "energy gap" and because Boltzmann statistics is satisfactory for the rotons. The previous relations (eq. (1)), with the constants appropriately adjusted, give very good qualitative agreement with the data from neutron scattering experiments (refs. 3 to 5) performed years after Landau's papers. Feynman (ref. 6) derived a similar energy spectrum from more basic principles, with an argument based on the Bose-Einstein statistics of He^4 atoms. Because Landau's derivation took no account of statistics, it made no qualitative distinction between He^4 and He^3 . Feynman's work is not entirely microscopic, however, for he utilizes the experimentally determined structure factor (ref. 7) for the liquid.

Two groups of experimenters (refs. 3 to 5) have measured the spectrum of elementary excitations in helium by neutron scattering experiments as proposed by Cohen and Feynman (ref. 8). The neutrons are scattered by density waves in the liquid. According to Pines (ref. 9), these density waves have the same energy spectrum as the elementary excitations for a system of bosons. The spectrum is shown in figure 1, and the phonon

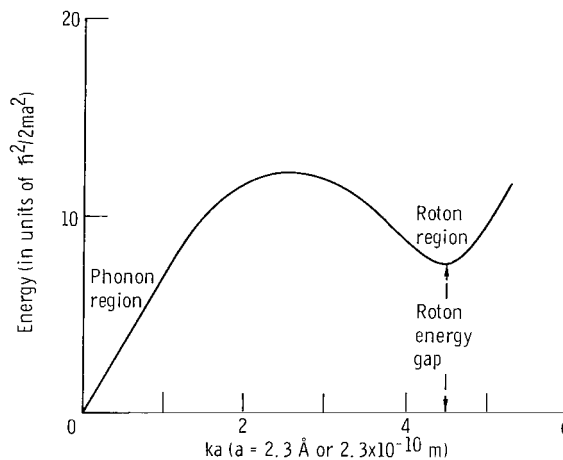


Figure 1. - The experimental spectrum.

and roton regions are identified there.

A chief aim of the many-body problem for helium is to derive this spectrum from the theoretically or experimentally determined interatomic forces of helium atoms, without further input from experiments. This work derives the spectrum from a realistic interparticle potential by combining three methods. First, a generalized or "smeared" Bose-Einstein condensation is assumed because the scattering length of the interparticle potential is negative. Second, a modified reaction matrix is introduced to handle the strong repulsive core of the helium potential. Third, a Thermodynamically Equivalent Hamiltonian (TEH) method permits the inclusion of all forward, exchange, and pair scattering interaction terms.

THE IMPERFECT BOSON GAS

The microscopic problem of the imperfect boson gas has been considered by numerous authors (refs. 10 to 23). The starting point is the second-quantized Hamiltonian for a system of bosons having an interparticle potential operator V

$$H = \sum_{\mathbf{k}} \frac{\hbar^2 \mathbf{k}^2}{2m} a_{\mathbf{k}}^+ a_{\mathbf{k}} + \frac{1}{2} \sum_{\mathbf{k}_1 \mathbf{k}_2 \mathbf{k}_3 \mathbf{k}_4} \langle \mathbf{k}_1 \mathbf{k}_2 | V | \mathbf{k}_3 \mathbf{k}_4 \rangle a_{\mathbf{k}_1}^+ a_{\mathbf{k}_2}^+ a_{\mathbf{k}_3} a_{\mathbf{k}_4} \quad (2)$$

(Symbols are defined in appendix A.) All indices are understood to be vectors, although the vector signs have been suppressed to avoid overcrowding. The system is enclosed in a box of volume Ω , and the summations run over all allowed free-particle states in the box. The operator $a_{\mathbf{k}}^+$ is the creation operator for a plane wave state with propagation vector $\vec{\mathbf{k}}$, and $a_{\mathbf{k}}$ is the corresponding destruction operator. The interaction potential $v(r)$ is a spherically symmetric function of the distance r between two atoms, and appears here in matrix elements with respect to free-particle two-body states, for example, $\langle \mathbf{k}_1 \mathbf{k}_2 | V | \mathbf{k}_3 \mathbf{k}_4 \rangle$. These elements can be expressed in terms of matrix elements with respect to one-particle states in a central potential by changing to center-of-mass coordinates. The result is

$$\langle \mathbf{k}_1 \mathbf{k}_2 | V | \mathbf{k}_3 \mathbf{k}_4 \rangle = \delta_{\mathbf{k}_1 + \mathbf{k}_2, \mathbf{k}_3 + \mathbf{k}_4} \hat{v}(\mathbf{k}_3 - \mathbf{k}_1) = \delta_{\mathbf{k}_1 + \mathbf{k}_2, \mathbf{k}_3 + \mathbf{k}_4} \hat{v}(\mathbf{q})$$

where $\mathbf{q} = |\vec{\mathbf{k}}_3 - \vec{\mathbf{k}}_1|$ is the momentum transfer, δ is the Kronecker delta, and $\hat{v}(\mathbf{q})$ is $1/\Omega$ times the three-dimensional Fourier transform of the real-space potential

$$\hat{v}(\mathbf{q}) = \frac{1}{\Omega} \int d^3\mathbf{r} e^{i\vec{q}\cdot\vec{r}} v(\mathbf{r})$$

In the present treatment, the change to center-of-mass coordinates must be postponed until after the K matrix is introduced. The form $\langle k_1 k_2 | V | k_3 k_4 \rangle$ will be retained until that point.

The diagonalization of the Hamiltonian (eq. (2)) has not been accomplished. Many authors drop most of the interaction terms, although attempting to keep as many as possible. These retained terms should be diagonalizable or amenable to some other treatment. One successful theory based on a "truncated" Hamiltonian is the Bardeen, Cooper, and Schrieffer theory of superconductivity (refs. 24 and 25).

The Hamiltonian to be used here is the "pair Hamiltonian" of Girardeau and Arnowitt (ref. 21). All interaction terms are neglected except the forward scattering, exchange scattering, and pair scattering terms. These three types of terms are represented in figure 2 and have the following second-quantized forms, $\langle qp | V | qp \rangle a_q^+ a_p^+ a_q a_p$, $\langle qp | V | pq \rangle a_q^+ a_p^+ a_p a_q$, and $\langle -qq | V | -pp \rangle a_{-q}^+ a_q^+ a_{-p} a_p$, respectively. The truncated Hamiltonian, now called the pair Hamiltonian H_p (ref. 21), has become

$$H_p = \sum_{\mathbf{k}} \frac{\hbar^2 \mathbf{k}^2}{2m} a_{\mathbf{k}}^+ a_{\mathbf{k}} + \frac{1}{2} \sum_{\mathbf{q}\mathbf{p}} \langle \mathbf{q}\mathbf{p} | V | \mathbf{q}\mathbf{p} \rangle a_{\mathbf{q}}^+ a_{\mathbf{p}}^+ a_{\mathbf{q}} a_{\mathbf{p}} + \frac{1}{2} \sum_{\substack{\mathbf{q}\mathbf{p} \\ \mathbf{q} \neq \pm \mathbf{p}}} \langle \mathbf{q}\mathbf{p} | V | \mathbf{p}\mathbf{q} \rangle a_{\mathbf{q}}^+ a_{\mathbf{p}}^+ a_{\mathbf{p}} a_{\mathbf{q}} + \frac{1}{2} \sum_{\substack{\mathbf{q}\mathbf{p} \\ \mathbf{q} \neq \mathbf{p}}} \langle -\mathbf{q}\mathbf{q} | V | -\mathbf{p}\mathbf{p} \rangle a_{-\mathbf{q}}^+ a_{\mathbf{q}}^+ a_{-\mathbf{p}} a_{\mathbf{p}} \quad (3)$$

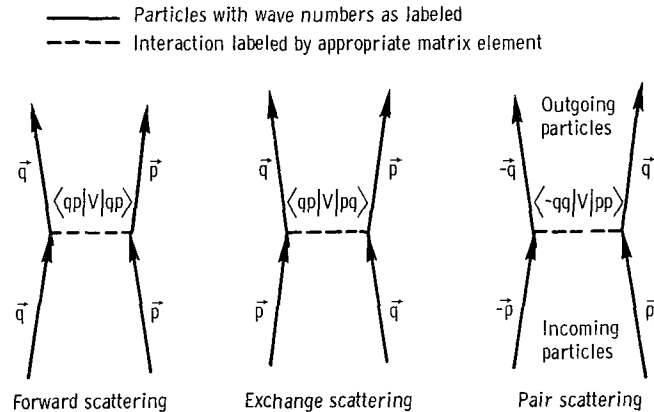


Figure 2. - Interaction terms retained in pair Hamiltonian.

The restrictions on the sums are necessary to prevent duplication of terms.

Even the simplified Hamiltonian (eq. (3)) has not been diagonalized. If two additional simplifications are made, diagonalization can be achieved: These are: (1) keep only those interaction terms containing at least two creation or annihilation operators with subscript zero; (2) approximate both a_0^+ and a_0 by \sqrt{N} . If the potential is repulsive, that is, $\hat{v}(0) > 0$, the resulting "Bogoliubov Hamiltonian" can be diagonalized (ref. 10). The second simplification, called the Bogoliubov approximation, is justified for weak interactions near absolute zero because nearly all particles are expected to be in the zero-momentum state. There is a canonical transformation on the single-particle operators which diagonalizes the Bogoliubov Hamiltonian. Such a transformation is called the Bogoliubov transformation and will be used later in the present work. A phonon spectrum for low momenta occurs in this approximation and a free-particle spectrum at high momenta. In the intermediate range of momenta the spectrum has a region connecting the linear and quadratic sections. For an appropriate repulsive potential this region could have the general shape of the roton region of the liquid helium spectrum. The model thus has two features resembling liquid helium: the low-momentum phonon spectrum and at least a hint of a roton region.

Girardeau and Arnowitt (ref. 10), using a variational method, consider the entire pair Hamiltonian (eq. (3)), without making the Bogoliubov approximation. Wentzel (ref. 14) and Luban (ref. 15), also studying the Hamiltonian (eq. (3)), allow thermal excitation, and find a simpler diagonalizable Hamiltonian which gives the same thermodynamics as that of equation (3). All three of these studies find an energy gap in the low-momentum excitation spectrum. That is, $E(0) = 0$, but $\lim_{k \rightarrow 0} E(k) \neq 0$. These results are for weak interparticle potentials with $\hat{v}(0) > 0$, and they assume that Bose-Einstein condensation takes place with particles "condensing" into the zero-momentum state. The spectrum of this pair Hamiltonian model, which includes more terms than the Bogoliubov Hamiltonian, is, nevertheless, further from that of helium II.

There are two important differences between the interparticle potential used in the aforementioned studies and the actual helium potential. First, the helium potential is much more strongly repulsive at close approach. Secondly, the scattering length for helium is negative.¹ (In fact, the scattering length is so negative that the atoms can almost form a two-body bound state.) For the Yntema-Schneider (Y. S.) potential (refs. 26 and 27), the scattering length is negative, and its magnitude is several times the repulsive core diameter. For a potential with a singular repulsive core, as in helium, the sign of the scattering length plays the role that the sign of $\hat{v}(0)$ plays in a weak potential, roughly

¹The scattering length characterizes the "net effect" of a potential, in that a positive scattering length indicates net repulsion, and negative scattering length indicates net attraction. The scattering length for hard spheres is equal to the diameter of a sphere.

speaking. Thus a system of atoms with negative scattering length may be expected to correspond more nearly to a system with $\hat{v}(0) < 0$ than to one with $\hat{v}(0) > 0$. The repulsive core and the negative scattering length each require changes from the methods used by the authors mentioned in the preceding paragraph.

THEORETICAL TECHNIQUES

Three main methods will now be described, which in combination allow a potential with singular repulsive core and an attractive well to be studied using the pair Hamiltonian. To deal with potentials with negative scattering length (like helium), a generalized or "smeared" Bose-Einstein condensation is assumed. To avoid the infinite matrix elements of the repulsive core, a type of reaction matrix is used in place of the potential. Finally to obtain a diagonalized form from the pair Hamiltonian, the Wentzel thermodynamically equivalent Hamiltonian (TEH) method is used. The three methods are discussed in the three following sections.

Generalized Bose-Einstein Condensation

Consider first the effect of having a potential with $\hat{v}(0) < 0$. Girardeau (refs. 22 and 23) argues that for weak attractive potentials, where $\hat{v}(0) < 0$, the lowest energy state is not one in which the zero-momentum state contains a finite fraction of the particles (simple Bose-Einstein condensation). It is rather one in which a large number of distinct low-momentum states contain a finite fraction of the particles but any single state contains only a negligibly small fraction. In this generalized condensation all states with momentum less than a cutoff momentum p_0 are assumed to have zero energy. A finite fraction of the particles occupy the group of states, but no single state, not even the $p = 0$ state, contains a finite fraction. The group of states containing condensed particles draws arbitrarily close to zero momentum and bears a deceptive resemblance to simple condensation. It is the fact that no single state is macroscopically occupied (that is, contains a finite fraction of the total particles) that distinguishes the two types of condensation.

In reference 17, the descriptive statements about generalized condensation are formulated as follows. As the thermodynamic limit is taken, that is, $N \rightarrow \infty$ but N/Ω is constant,

$$\Omega \rightarrow \infty$$

$$p_0 = O(\Omega^{-z}) \quad (z > 0)$$

$$\langle a_p^+ a_p \rangle = O(\Omega^z(p)) \quad \text{for } |p| < p_0 \text{ and } 0 < z(p) = O(1) < 1$$

and

$$\sum_{p < p_0} \langle a_p^+ a_p \rangle = O(\Omega)$$

The results of three studies support the use of a smeared condensation. Girardeau demonstrates by variational means that smearing gives a lower energy for weakly attractive systems than does a simple condensation. Sawada and Vasudevan (ref. 28) show in a simplified model with negative scattering length that the states into which the particles condense should be a combination of zero- and nonzero-momentum states. This combination of states may be viewed as a smeared condensation.

Additional incentive to investigate the smeared type of condensation is provided by the work of Luban (appendix E of ref. 17). He showed that in the pair Hamiltonian model with a hard core pseudopotential and weak attractive interactions, a smeared condensation leads to a phonon-like spectrum for low-momentum excitations rather than to the energy gap predicted by simple condensation. The modifications to be made below to treat strong potentials do not change the character of these low-momentum excitations if the scattering length is negative. Thus it appears reasonable to use a smeared condensation in a study of helium, which has a negative scattering length.

The Reaction Matrix

To treat an interparticle potential with a strong repulsive core, the pair Hamiltonian (eq. (3)) is inadequate as it stands. The matrix elements of the interaction potential that appear in equation (3) are arbitrarily large for arbitrarily strong cores. This is easily seen by considering a repulsive core of uniform height V_0 and radius a as shown in figure 3. Then

$$\langle k_1 + q, k_2 - q | v | k_1 k_2 \rangle = \hat{v}(q) = \frac{4\pi V_0}{\Omega q} \int_0^a r \sin(qr) dr$$

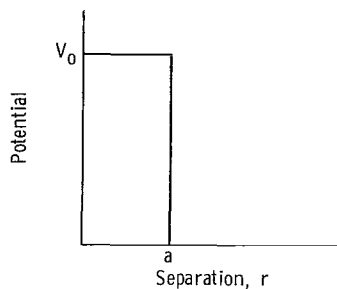


Figure 3. - Square repulsive core.

This general matrix element is proportional to V_0 . In the limit of $V_0 \rightarrow \infty$ (hard core), progress can still be made by summing enough terms in a many-body perturbation series of the exact Hamiltonian to obtain a finite result.

The method used here to effect this summing is similar to that of Brueckner and Sawada (refs. 14 and 15). The matrix elements of the interparticle potential operator are replaced by the elements of a type of reaction matrix. Since the reaction matrix K is defined by

$$K = V + VGK \quad (4)$$

where V is the exact two-body potential operator and G is a Green's function operator, it has an expansion of the form

$$K = V + VGV + VGVGV + \dots$$

The use of matrix elements of K in place of matrix elements of V (which is the first term in the expansion of K) brings many more interaction terms into the Hamiltonian without complicating its form. If the matrix elements of K are calculable from V , then the use of K elements effectively presumes enough interaction terms to give a finite result. (Note that, for very weak V , the K operator approaches V but that, for singular core potentials, elements of K with respect to plane waves are still finite whereas those of V are infinite (refs. 12 and 13).)

The arguments for this replacement of V by K and the selection of the operator G are made in appendix B by considering the many-body perturbation expansion of the free energy. The perturbation expansion of the free energy based on the pair Hamiltonian containing K 's instead of V 's is more nearly like the expansion of the free energy based on a complete nontruncated Hamiltonian. The operator G must be appropriately chosen, however. The argument in appendix B shows that $G = -1/H_0$, where H_0 is the kinetic energy operator, can be used.

Matrix elements of K with respect to two-body plane-wave states are needed to insert into the truncated Hamiltonian. To reduce the calculation of the matrix elements to manageable proportions, an approximation is made - the center-of-mass approximation. The matrix elements of K with respect to two-body states are approximated by elements with respect to one-body center-of-mass states. Details of the center-of-mass approximation, the types of matrix elements needed, and the decomposition of the elements into partial waves are contained in appendixes C and D. The important results from appendixes B, C, and D are the following:

- (1) Matrix elements $\langle kp|V|qr\rangle$ in the Hamiltonian are to be replaced by the corresponding reaction matrix elements $\langle kp|K|qr\rangle$.
- (2) The two-body elements $\langle kp|K|qr\rangle$ are to be approximated by the one-body center-of-mass elements

$$\left\langle \frac{k-p}{2} |K| \frac{q-r}{2} \right\rangle$$

The integral equation $K = V + VGK$ for these one-body elements is decomposed into a similar equation for each partial wave by expanding all elements of the matrices in spherical harmonics. The integral equation for each partial wave can be solved by machine. Only even partial waves are needed, and three of these give sufficient accuracy in the energy spectrum from zero momentum to just past the roton minimum.

The Thermodynamically Equivalent Hamiltonian

The modification of the truncated Hamiltonian (eq. (3)) to allow treatment of strongly repulsive cores has not changed its basic form. It is still of the type which can be treated by the TEH method (refs. 13 and 14). In the first part of this section the meaning of "thermodynamically equivalent" is discussed, and especially the question of how this method can be applied in the present work where the use of the reaction matrix is justified only in the limit as $T \rightarrow 0$ (appendix B).

The essence of the Wentzel method is that a simpler Hamiltonian than equation (3) can be found which gives the same partition function as equation (3) in the limit as $\Omega \rightarrow \infty$ (the thermodynamic limit) but which can be exactly diagonalized by the Bogoliubov transformation.² Two systems with the same partition function have exactly the same thermodynamics, but, in general, this does not guarantee any microscopic similarity. The microscopic similarity is a central point of this work, however, which attempt to

²Note that the Bogoliubov transformation and the Bogoliubov approximation are distinct.

find the energy spectrum of elementary excitations (normal modes) in a dense boson gas resembling helium. The relation, if any, between the spectrum of excitations found by diagonalizing the thermodynamically equivalent Hamiltonian and the experimentally determined spectrum of excitations (refs. 3 to 5) for liquid helium must be examined.

The grand partition function of a general interacting system is

$$\mathcal{Q}(\beta, \mu) = \sum_{\text{all distinguishable states}} e^{-\beta(E_{\text{state}} - \mu N_{\text{op}})}$$

where N_{op} is the total number operator. If the system Hamiltonian (eq. (3)) could be diagonalized so it could be written as

$$H = \sum_{\mathbf{k}} E_{\mathbf{k}} \alpha_{\mathbf{k}}^+ \alpha_{\mathbf{k}}$$

where $\alpha_{\mathbf{k}}^+$ creates $|\mathbf{k}\rangle$, a state with momentum \mathbf{k} and energy $E_{\mathbf{k}}$, then the grand partition function would be

$$\mathcal{Q}(\beta, \mu) = \sum_{\{\mathbf{n}_{\mathbf{k}}\}} e^{-\beta \sum_{\mathbf{k}} (E_{\mathbf{k}} - \mu) n_{\mathbf{k}}} \equiv \sum_{\{\mathbf{n}_{\mathbf{k}}\}} e^{-\beta \sum_{\mathbf{k}} \epsilon_{\mathbf{k}} n_{\mathbf{k}}} \quad (5)$$

where $\sum_{\{\mathbf{n}_{\mathbf{k}}\}}$ indicates a sum over all possible sets of occupation numbers $n_{\mathbf{k}}$. The energies $E_{\mathbf{k}}$ in this last expression are temperature independent numbers. The Wentzel method diagonalizes the truncated Hamiltonian (eq. (3)) in the sense that

$$\mathcal{Q}(\beta, \mu) = \sum_{\{n_k\}} e^{-\beta \sum_k \epsilon_k(\beta) n_k} \quad (6)$$

Here, as in equation (5), the summation runs over all sets of occupation numbers n_k . This partition function (eq. (6)) is constructed equal to that of equation (5) for any β , but in general $\epsilon_k(\beta)$, a function of temperature, bears no simple relation to ϵ_k of equation (5). If, however, for a range of temperature from zero to some finite temperature T_f , $\epsilon_k(\beta)$ is independent of temperature, then it is expected that

$$\epsilon_k(\beta) = E_k - \mu = \epsilon_k$$

for $T < T_f$.

The integral equations that determine $\epsilon_k(\beta)$ are not very sensitive to temperature near $T = 0$ because temperature enters only in the thermal expectation values of the number operator $\langle a_k^\dagger a_k \rangle$ and of the pair destruction operator $\langle a_k a_{-k} \rangle$. These will have limiting and, in general, nonzero values as $T \rightarrow 0$. For very small T , departures from the limiting values will be arbitrarily small. The reason for this can be most easily seen after the solutions of the equations are obtained. The lowest energy excitations are seen to be phonon-like, that is, their energies are proportional to momentum. This type of excitation spectrum is much more "rigid" against thermal excitation than, for example, a quadratic free-particle spectrum. In the former case many fewer states have energies of the order of kT than in the latter case. The relative rigidity against excitations causes the number of excited particles to be relatively constant near zero temperature. This, in turn, leads to the insensitivity to temperature of the excitation spectrum and all thermal expectation values as $T \rightarrow 0$. Thus the phonon-like spectrum leads to the temperature independence of $\epsilon_k(\beta)$ as $\beta \rightarrow \infty$ ($T \rightarrow 0$) and hence to the assertion that the $\epsilon_k(\beta \rightarrow \infty)$ found by Wentzel's method is the same as the ϵ_k normal mode spectrum.

As previously mentioned, the experimentally determined excitation spectrum is not strictly temperature independent in the temperature range 1.1 to 1.8 K. The roton minimum is 5 percent lower in energy at 1.8 K than at 1.1 K. It is therefore questionable whether the experiment measures purely normal (noninteracting) modes, or perhaps whether strictly normal modes even exist. However, the temperature dependence is not strong, and at least part of it may be due to the slight change in density, so the modes measured experimentally are, at worst, weakly interacting.

INTEGRAL EQUATIONS FOR THE SPECTRUM

Consider again the pair Hamiltonian (eq. (3)), replacing the V-matrix elements with the corresponding K-matrix elements to yield the following:

$$\begin{aligned}
 H_p &= \sum_k \left(\frac{\hbar^2 k^2}{2m} - \mu \right) a_k^+ a_k + \frac{1}{2} \sum_{pq} \langle qp | K | qp \rangle a_q^+ a_p^+ a_q a_p \\
 &\quad + \frac{1}{2} \sum_{\substack{pq \\ p \neq \pm q}} \langle pq | K | qp \rangle a_p^+ a_q^+ a_q a_p + \frac{1}{2} \sum_{pq} \langle -qq | K | -pp \rangle a_{-q}^+ a_q^+ a_{-p} a_p \\
 &= \sum_k \left(\frac{\hbar^2 k^2}{2m} - \mu - \frac{K_{kkkk}}{2} \right) a_k^+ a_k + \frac{1}{2} \sum_{\substack{qp \\ q \neq p}} K_{qpqp} a_q^+ a_q a_p^+ a_p \\
 &\quad + \frac{1}{2} \sum_{\substack{pq \\ p \neq \pm q}} K_{pqqp} a_p^+ a_q^+ a_q a_p + \frac{1}{2} \sum_{\substack{pq \\ p \neq q}} K_{-qq-pp} a_{-q}^+ a_q^+ a_{-p} a_p \quad (7)
 \end{aligned}$$

where $K_{pqrs} \equiv \langle pq | K | rs \rangle$. (Note that $\frac{1}{2} \sum_{pq} K_{qpqp} a_q^+ a_p^+ a_q a_p = \frac{1}{2} \sum_{pq} K_{qpqp} a_q^+ a_q a_p^+ a_p -$

$\frac{1}{2} \sum_k K_{kkkk} a_k^+ a_k$.) The form (eq. (7)) can be treated by the TEH method (ref. 13). As in Luban's version (ref. 14) of Wentzel's method, μ , the chemical potential, has been inserted in H_p . This is soon eliminated from the equations.

To find the TEH, first define new operators B_k , B_k^+ , C_k , and C_k^+ in the following way

$$a_k^+ a_k \equiv B_k + \xi_k$$

$$a_{-k} a_k \equiv C_k + \eta_k$$

where the values of the real c-numbers ξ_k and η_k will be chosen to eliminate some terms from the new equivalent Hamiltonian. These substitutions give

$$H_p = \sum_k \left(\frac{\hbar^2 k^2}{2m} - \mu - \frac{K_{kkkk}}{2} \right) a_k^+ a_k + \frac{1}{2} \sum_{pq} K_{qpqp} (B_p + \xi_p)(B_q + \xi_q) \\ + \frac{1}{2} \sum_{\substack{pq \\ p \neq q}} K_{pqqp} (B_q + \xi_q)(B_p + \xi_p) + \frac{1}{2} \sum_{\substack{pq \\ p \neq q}} K_{-qq-pp} (C_q^+ + \eta_q)(C_p + \eta_p)$$

Because $B_k^+ = B_k$,

$$H_p = \sum_k \left(\frac{\hbar^2 k^2}{2m} - \mu - \frac{K_{kkkk}}{2} \right) a_k^+ a_k + \frac{1}{2} \sum_{pq} K_{qpqp} [B_p^+ B_q + \xi_p (a_q^+ a_q - \xi_q) \\ + (a_p^+ a_p - \xi_p) \xi_q + \xi_p \xi_q] + \frac{1}{2} \sum_{\substack{pq \\ p \neq q}} K_{pqqp} [B_q^+ B_p + \xi_q (a_p^+ a_p - \xi_p) + (a_q^+ a_q - \xi_q) \xi_p + \xi_p \xi_q] \\ + \frac{1}{2} \sum_{\substack{pq \\ p \neq q}} K_{-qq-pp} [C_q^+ C_p + \eta_q (a_p a_{-p} - \eta_p) + (a_q^+ a_{-q}^+ - \eta_q) \eta_p + \eta_p \eta_q]$$

Note $K_{qpqp} = K_{pqqp}$ and $K_{ppqp} = K_{qqpp}$; that is, the reaction matrix element is symmetric with respect to interchange of the first and second pairs of indices. Using these facts and manipulating the dummy indices yield

$$\begin{aligned}
H_p = \sum_k \left(\frac{\hbar^2 k^2}{2m} - \mu - \frac{K_{kkkk}}{2} \right) + \frac{1}{2} \sum_{pq} K_{qpqp} (B_p^\dagger B_q + 2\xi_p a_q^\dagger a_q - \xi_p \xi_q) \\
+ \frac{1}{2} \sum_{\substack{pq \\ p \neq \pm q}} K_{qppq} (B_q^\dagger B_p - 2\xi_p a_q^\dagger a_q + \xi_p \xi_q) \\
+ \frac{1}{2} \sum_{\substack{pq \\ p \neq q}} K_{-qq-pp} [C_q^\dagger C_p + \eta_p (a_q^\dagger a_{-q}^\dagger + a_q a_{-q}) - \eta_q \eta_p]
\end{aligned}$$

Now collect the terms into two groups, putting those containing B , B^\dagger , C , and C^\dagger into

$$H_1 = \frac{1}{2} \sum_{qp} K_{qpqp} B_p^\dagger B_q + \frac{1}{2} \sum_{\substack{pq \\ p \neq \pm q}} K_{qppq} B_q^\dagger B_p + \frac{1}{2} \sum_{\substack{pq \\ p \neq \pm q}} K_{-qq-pp} C_q^\dagger C_p$$

All the other terms are put into

$$\begin{aligned}
H_{TE} = U + \sum_k \left(\frac{\hbar^2 k^2}{2m} - \mu - \frac{K_{kkkk}}{2} \right) a_k^\dagger a_k + \sum_{qp} K_{qpqp} \xi_p a_q^\dagger a_q \\
+ \sum_{\substack{qp \\ q \neq \pm p}} K_{qppq} \xi_p a_q^\dagger a_q + \frac{1}{2} \sum_{\substack{qp \\ q \neq p}} K_{-qq-pp} \eta_p (a_q^\dagger a_{-q}^\dagger + a_q a_{-q})
\end{aligned}$$

where

$$U = -\frac{1}{2} \sum_{qp} K_{qpqp} \xi_p \xi_q - \frac{1}{2} \sum_{\substack{pq \\ p \neq \pm q}} K_{qppq} \xi_p \xi_q - \frac{1}{2} \sum_{\substack{qp \\ q \neq p}} K_{-qq-pp} \eta_p \eta_q$$

which is a c-number. Let

$$f_k = \frac{\hbar^2 k^2}{2m} - \mu - \frac{K_{kkkk}}{2} + \sum_p K_{kpkp} \xi_p + \sum_{p \neq \pm k} K_{kppk} \xi_p$$

and

$$h_k = \sum_{p \neq k} K_{-kk-pp} \eta_p$$

(8)

Then

$$H_{TE} = U + \sum_k f_k a_k^+ a_k + \frac{1}{2} \sum_k h_k (a_k^+ a_{-k}^+ + a_k a_{-k})$$

(9)

According to Wentzel's TEH method, H_{TE} will lead to the same thermodynamic properties as H_P if ξ_p and η_p are chosen as $\xi_p = \langle a_p^+ a_p \rangle$ and $\eta_p = \langle a_p^+ a_{-p}^+ \rangle = \langle a_{-p} a_p \rangle$, where the bracket denotes an average with respect to the grand ensemble. It has been shown that the Wentzel result remains valid for the "Hamiltonian" which has resulted from replacement of V-matrix elements by K-matrix elements.

In appendix E the Bogoliubov transformation is used to diagonalize equation (9), the result being

$$H_{TE} = U_0 + \sum_k \epsilon_k \alpha_k^+ \alpha_k$$

(10)

where

$$U_0 = U + \sum_k \frac{1}{2} (\epsilon_k - f_k)$$

and

$$\epsilon_k = \sqrt{f_k^2 - h_k^2}$$

(11)

It is noted in appendix E that the Bogoliubov transformation is not valid for any k for which $\epsilon_k = 0$. In a smeared condensation there is a group of states with $\epsilon_k = 0$, but these states are grouped arbitrarily close to $k = 0$ in the limit of infinite system volume. That is, these states all have wave numbers less than an arbitrarily small cutoff wave number p_0 . All the equations are to be solved only in the limit of infinite volume. Thus the Bogoliubov transformation can be performed for all states not in the condensate, that is, that have finite momenta in the volume limit. The generalized or smeared Bose-Einstein condensate exists in states with $\epsilon = 0$, and it is not necessary to perform any transformation to find the energy of these states. The number of particles in these states is found by taking the difference between the number residing in excited states and the total number.

In equations (8) the limit as k approaches zero gives (denoting $\lim_{k \rightarrow 0} f(k)$ as $f(0)$ and $\lim_{k \rightarrow 0} h(k)$ as $h(0)$)

$$\left. \begin{aligned} f(0) &= -\mu - \frac{1}{2} K_{0000} + \sum_p K_{0pop} \xi_p + \sum_{p \neq 0} K_{oppo} \xi_p \\ h(0) &= \sum_{p \neq 0} K_{oo-pp} \eta_p \end{aligned} \right\} \quad (12)$$

Because $\epsilon(0) = \sqrt{f^2(0) - h^2(0)} = 0$, $f(0) = \pm h(0)$. Paralleling Luban (ref. 15), let $f(0) = -h(0)$. Then μ can be eliminated from equations (8) using equations (12)

$$\begin{aligned} -\mu &= \frac{1}{2} K_{0000} - \sum_p K_{0pop} \xi_p - \sum_{\substack{p \\ p \neq 0}} K_{oppo} \xi_p - \sum_{\substack{p \\ p \neq 0}} K_{oo-pp} \eta_p \\ &= \frac{1}{2} K_{0000} - K_{0000} \left[\sum_{p < p_0} \xi_p + \sum_{\substack{p < p_0 \\ p \neq 0}} (\xi_p + \eta_p) \right] - \sum_{p > p_0} K_{0pop} \xi_p \\ &\quad - \sum_{p > p_0} K_{oppo} \xi_p - \sum_{p > p_0} K_{oo-pp} \eta_p \end{aligned}$$

Then equations (8) become

$$f_k = \frac{\hbar^2 k^2}{2m} + \sum_{p < p_0} \xi_p (K_{koko} + K_{kook} - K_{oooo}) - K_{oooo} \sum_{\substack{p < p_0 \\ p \neq 0}} (\xi_p + \eta_p) \\ + \sum_{p > p_0} (K_{pkpk} + K_{pkkp} - K_{popo} - K_{poop}) \xi_p - \sum_{p > p_0} K_{oop-p} \eta_p \\ h_k = \sum_{p < p_0} K_{k-koo} \eta_p + \sum_{\substack{p > p_0 \\ p \neq k}} K_{k-kp-p} \eta_p$$

where terms with $p < p_0$ are separated from the sums, and continuity of the K-matrix elements near zero momenta with respect to any of the indices is used. Two terms, $K_{oooo}/2$ and $-K_{kkkk}/2$, have been dropped from f_k because they cancel in the center-of-mass approximation as can be seen from appendix C.

It was shown by Luban (ref. 15) that (in the thermodynamic limit) as $p \rightarrow 0$, $\eta_p \rightarrow \xi_p + \frac{1}{2}$. Then since $\xi_p = \langle a_p^+ a_p \rangle$, the sums $\sum_{p < p_0} \xi_p$ and $\sum_{p < p_0} \eta_p$ are merely the grand ensemble averages of the number of particles in the "smeared" condensate. If this number is N_0 and the sums are replaced by integrals by letting

$$\sum_p \rightarrow \frac{\Omega}{(2\pi)^3} \int d^3 p$$

then

$$f_k = \frac{\hbar^2 k^2}{2m} + N_0 (K_{koko} + K_{kook} - 3K_{oooo}) + \frac{\Omega}{(2\pi)^3} \int \{ [K_{pkpk} + K_{pkkp} - K_{popo} - K_{poop}] \xi_p \\ - K_{oop-p} \eta_p \} d^3 p$$

$$h_{\mathbf{k}} = N_0 K_{\mathbf{k}-\mathbf{k}00} + \frac{\Omega}{(2\pi)^3} \int K_{\mathbf{k}-\mathbf{k}\mathbf{p}-\mathbf{p}} \eta_{\mathbf{p}} d^3p$$

Note that in the integral form it is permissible to ignore the restrictions $p \neq k$, $p \neq \pm k$, and $p > p_0$ and to carry out the integrals throughout p -space. The first two restrictions do not affect the integration since the excluded discrete states, $p = k$ or $p = \pm k$, make negligible contributions. In the thermodynamic limit p_0 is assumed to approach zero, and the interval of integration that would be excluded by the last restriction makes a negligible contribution.

From appendix E,

$$\xi_{\mathbf{k}} = \frac{1}{2} \left[\frac{f_{\mathbf{k}}}{\epsilon_{\mathbf{k}}} \coth \left(\frac{\beta \epsilon_{\mathbf{k}}}{2} \right) - 1 \right] \quad \text{and} \quad \eta_{\mathbf{k}} = -\frac{1}{2} \frac{h_{\mathbf{k}}}{\epsilon_{\mathbf{k}}} \coth \left(\frac{\beta \epsilon_{\mathbf{k}}}{2} \right)$$

The one remaining relation needed is $N = \sum_{\mathbf{k}} \langle a_{\mathbf{k}}^+ a_{\mathbf{k}} \rangle = \sum_{\mathbf{k}} \xi_{\mathbf{k}}$ or

$$N_0 = N - [\Omega/(2\pi)^3] \int \xi_{\mathbf{k}} d^3k. \quad ^3$$

These equations constitute a set of nonlinear coupled integral equations. Once the necessary elements of the reaction matrix K are calculated, the equations may be solved numerically for $\epsilon(\mathbf{k})$, the quasiparticle energy spectrum, and for N_0/N , the fraction of particles (not quasiparticles) in the condensate.

It is convenient for machine solution (and for simplicity of form) to nondimensionalize the integral equations. This can be done by making the following definitions:

$$x \equiv ka \quad y \equiv pa \quad \gamma \equiv \frac{r}{a}$$

$$F(x) \equiv \frac{2ma^2}{\hbar^2} f_{\mathbf{k}} \quad H(x) \equiv \frac{2ma^2}{\hbar^2} h_{\mathbf{k}} \quad E(x) \equiv \frac{2ma^2}{\hbar^2} \epsilon_{\mathbf{k}}$$

$$P \equiv \frac{N}{\Omega} a^3 \quad P_0 \equiv \frac{N_0}{\Omega} a^3 \quad B \equiv \frac{\hbar^2}{2ma^2} \frac{1}{kT}$$

³Here it is implicitly intended that, for $p < p_0$, ξ_p and η_p inside integral signs mean simply the smooth extrapolations from $p > p_0$. The actual values of ξ_p and η_p for $p < p_0$ are much larger and their contributions have been separated out already.

$$\mathcal{K}_{pqrs} \equiv \frac{\Omega}{8\pi} \frac{2m}{\hbar^2 a} K_{pqrs} \quad \mathcal{V}(\gamma) \equiv \frac{ma^2}{\hbar^2} v(r)$$

where a is any reference dimension, taken to be 2.3 \AA ($2.3 \times 10^{-10} \text{ m}$), the approximate core size (fig. 16), in this work. In these dimensionless quantities, the equations are

$$\left. \begin{aligned} F(x) &= x^2 + 8\pi P_0 (\mathcal{K}_{xoxo} + \mathcal{K}_{xoox} - 3\mathcal{K}_{oooo}) \\ &+ \frac{1}{\pi^2} \int d^3y \xi_y (\mathcal{K}_{xyxy} + \mathcal{K}_{xyyx} - \mathcal{K}_{yoyo} - \mathcal{K}_{yooy}) - \frac{4}{\pi} \int_0^\infty y^2 dy \mathcal{K}_{ooy-y} \eta_y \\ H(x) &= 8\pi P_0 \mathcal{K}_{x-xoo} + \frac{4}{\pi} \int_0^\infty y^2 dy \mathcal{K}_{x-xy-y} \eta_y \\ E(x) &= \sqrt{F^2(x) - H^2(x)} \\ P_0 &= P - \frac{1}{2\pi^2} \int_0^\infty \xi_y y^2 dy \end{aligned} \right\} \quad (13)$$

As discussed in appendix C a general element K_{xyzu} of the reaction matrix is approximated in this work by the one-particle, center-of-mass reaction matrix element $\frac{K_{x-y} z-u}{2 \quad 2}$. Hence, in calculations K_{xoxo} is replaced by $\frac{K_{x \quad x}}{2 \quad 2}$, for example. The equations for the one-particle reaction matrix elements, derived in appendix D, are these

$$\langle \vec{k} | \mathbf{K} | \vec{p} \rangle = \sum_l (2l+1) P_l(\hat{k} \cdot \hat{p}) \langle k | \mathbf{K} | p \rangle_l$$

where

$$\langle k | \mathcal{X} | p \rangle_l = \langle k | \mathcal{V} | p \rangle_l - \frac{2}{\pi} \int_0^\infty d(qa) \langle k | \mathcal{V} | q \rangle_l \langle q | \mathcal{X} | p \rangle_l \quad (D6)$$

and

$$\langle \mathbf{k} | \mathcal{V} | \mathbf{q} \rangle_L \equiv \int_0^\infty \gamma^2 \mathcal{V}(\gamma) j_L(ka\gamma) j_L(pa\gamma) d\gamma \quad (\text{D7})$$

Equations (13) are coupled and nonlinear but can be solved by relatively simple numerical methods on a computer. The same basic method is used as for solving the reaction matrix integral equation. Although the equations for F , H , and E are coupled and nonlinear, their solution is less demanding of machine computing time and memory storage than the solution of the linear reaction matrix equation (eq. (D6)). One reason is that F , H , and E are only one-dimensional arrays as compared to the two-dimensional \mathcal{X}_{xy} and require two orders of magnitude less storage. Secondly, the integrands in the F , H , and E equations vanish much more rapidly with large momentum and the numerical integration may be stopped sooner.

The method of solution is to start with a reasonable guess for the functions $F(ka)$, $H(ka)$, $E(ka)$, and $P_0 = P$ and to insert these quantities in the right-hand members of equations (13). The new values for the functions calculated by doing the integrals were then averaged with the original guesses, the result being used as the next approximation. With a reasonable initial guess, this iterative method converged to within a fraction of 1 percent in about ten iterations. The reason for averaging new values with old ones was to prevent oscillations around the actual solution.

Because all the integrands decrease very rapidly after the roton minimum is passed, it is necessary to carry the integration only to $p/\hbar \approx 4 \text{ \AA}^{-1}$ ($4 \times 10^{10} \text{ m}^{-1}$). (The roton minimum is observed experimentally at $p/\hbar = 1.8 \text{ \AA}^{-1}$ or $1.8 \times 10^{10} \text{ m}^{-1}$.)

THE INTERPARTICLE POTENTIAL

To solve the integral equations numerically, a specific potential function $v(r)$ must be chosen. The results presented in the next section will show great sensitivity to the strength of the potential well. Unfortunately, the well region has not been determined accurately by either experiment or theory. Consequently two potentials are presented in this section. They both fit the measured virial coefficients. One is an accepted potential; the other is constructed simply to illustrate the effect of a weaker attractive well.

Probably the best known expressions for the helium potential are the Slater-Kirkwood potential (ref. 29)

$$v(r) = (770e^{-4.6r} - 1.49 r^{-6}) \times 10^{-12} \quad (\text{14})$$

and the Yntema-Schneider (Y. S.) potential (ref. 27)

$$v(r) = (1200e^{-4.72r} - 1.24 r^{-6} - 1.89 r^{-8}) \times 10^{-12} \quad (15)$$

where $v(r)$ is in ergs and r is in angstroms. The Y.S. potential is shown in figure 4.

The former was derived on theoretical grounds. The attractive tail is calculated from second-order perturbation theory for the Van der Waals interaction of two neutral atoms. The form of the repulsive core, due to Slater (ref. 30), is a first approximation to the overlap energy of two atoms which are close together. The attractive part dominates for large interparticle separation and the repulsive part for very small separation. The potential for intermediate separations, in particular in the vicinity of the minimum of the potential well, is not determined with any great accuracy, but in fact is the result of adding the repulsive and attractive terms together in the range of intermediate separation.

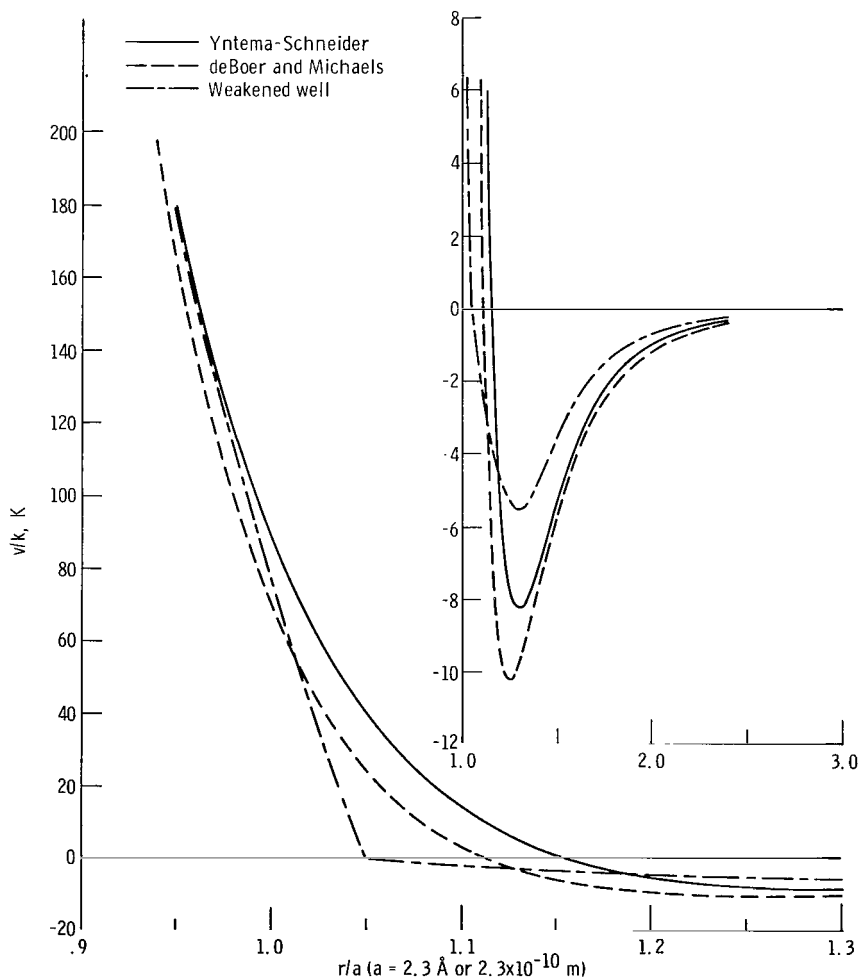


Figure 4. - Comparison of potentials.

The Y. S. potential was derived from experimental measurements of the second virial coefficient between 273 and 1473 K (ref. 26). The form $ae^{-br} - cr^{-6} - dr^{-8}$ was assumed. The value for c was taken from a theoretical derivation of London (ref. 31) and the value of d from Margenau (ref. 32), who calculated it to correspond to the London value of c . The values of a and b were then chosen to give a reasonable fit to the experimentally determined virial coefficients.⁴ This was done by calculating the second virial coefficient classically from

$$B(T) = 2\pi\eta_0 \int_0^{\infty} [1 - e^{-v(r)/kT}] r^2 dr \quad (16)$$

using various values of a and b to see what combination produced the best agreement between the calculated and experimental $B(T)$. Figures 5 and 6 show $B(T)$ calculated from equation (16) and using $v(r)$ from equation (15) and also show experimental data (refs. 27 and 35). The Slater-Kirkwood potential gives values of $V(T)$ that are up to 8 percent too low in the range 273 to 1473 K. It will not be used further here.

Virial coefficients for helium at high temperatures (>500 K) are very insensitive to the attractive part of the potential. Even at lower temperatures (down to approximately 80 K), the shape and depth of the well are inaccurately determined by a virial coefficient fit. Thus the attractive well is not accurately determined by the fit of Yntema and Schneider. In equation (15) just as in equation (14), the values of potential in the region of the well result from extrapolation of the limiting forms for larger and smaller r .

The well cannot, in fact, be accurately determined by matching virial coefficients using the classical formula (eq. (16)). At temperatures where $B(T)$ is sensitive to the well shape and depth, a quantum mechanical calculation of $B(T)$ must be made. Figure 6 shows an example of the inadequacy of the classical formula. It contains $B(T)$ as calculated from equation (16) and quantum mechanical calculations taken from reference 36. (The 6-12 potential used for the example is from ref. 37. It does not fit the high-temperature coefficients very well. For that reason it is used here only to contrast classical and quantum results for $B(T)$.) The quantum mechanical calculation of $B(T)$ is much more difficult and lengthy than the classical, and this apparently has prevented a quantum mechanical determination of the potential well.

⁴It is worth mentioning that London (ref. 33) and Brueckner and Gammel (ref. 34) have erroneously reported the Y. S. potential with the constant b given as 4.82. This value yields virial coefficients that are as much as 10 percent too low (between 273 and 1473 K) whereas $b = 4.72$ gives $B(T)$ to within 4 percent (and for most T within 1 percent) of the measured values. The erroneous value of b yields a potential that is too attractive.

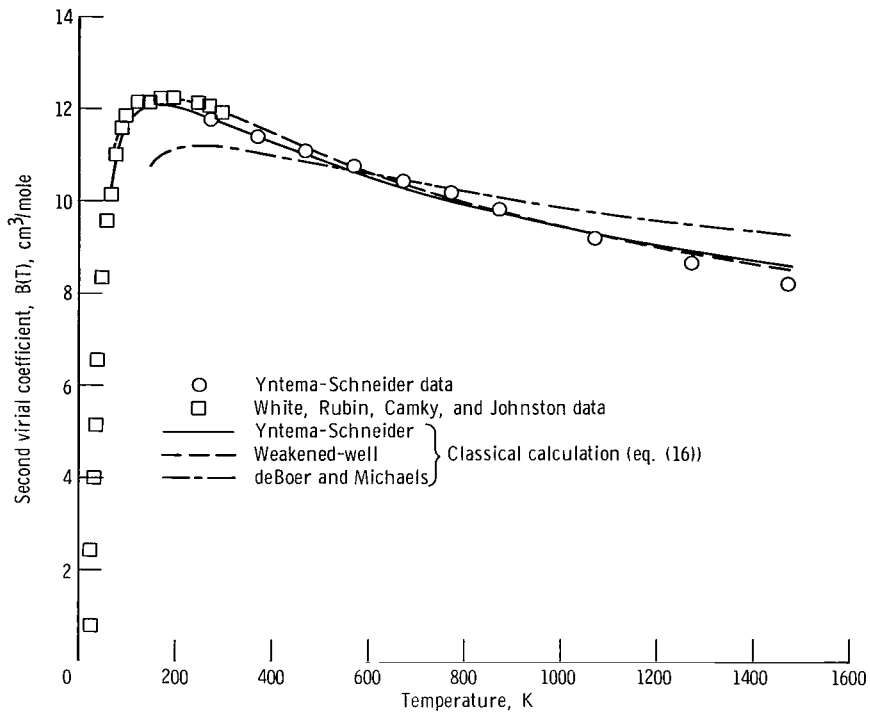


Figure 5. - Second virial coefficient for helium.

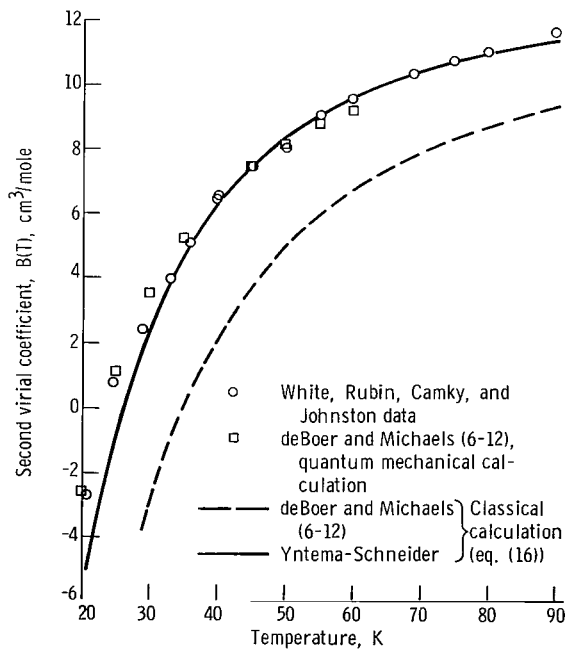


Figure 6. - Second virial coefficient for various potentials.

In spite of the inadequacy of the classical formula (eq. (16)), another potential has been constructed (by the classical eq. (16)) which fits the experimentally measured coefficients above 100 K as well as the Y. S. potential does). This new potential has a weaker well than that of Y. S. and a different core shape. It is introduced here simply to show that another potential can give a classical fit to $B(T)$ and yet yield (in the next section) an energy spectrum in much better agreement with the experiment. The new potential will be designated as the "weakened-well" potential and is shown in figure 4. The classical $B(T)$ calculated from it are shown in figure 5.

Two more potentials are used in the next section to further illustrate the effects of a shallower attractive well. These two potentials are identical with the Y. S. potential for $v(r) > 0$ but for $v(r) < 0$ are equal to $\alpha v_{Y.S.}(r)$, where α is chosen as 0.6 for one potential and 0.8 for the other.

Therefore, a total of four potentials will be used in the next section. Two of these, the Y. S. potential and the weakened-well potential, give good fits of the classically calculated virial coefficients to the experimental ones. The other two potentials with uniformly reduced wells are simply artificial potentials used to show the effects of gradually reducing the attractive well.

CALCULATED SPECTRA

The integral equations (eqs. (13)) have been solved numerically for each of the four potentials: the Y. S. potential, the weakened-well potential of figure 4, and the two potentials derived from the Y. S. by reducing the well by factors of 0.6 and 0.8. The resulting spectra are presented in this section beginning with the spectrum from the Y. S. potential. The qualitative features of that spectrum will be seen to be correct. The energies of all excitations will be seen to be high, however, and simple arguments will indicate that shallower wells should give better results. The spectrum corresponding to the weakened-well potential (which was shown to fit virial coefficient measurements) will be seen to be much better but still too high in energy. Lastly, the results for the uniformly reduced wells of 0.8 and 0.6 of Y. S. values are given.

The partial wave components of the reaction matrix were calculated from equations (D6) and (D7) as the first step in finding the spectrum. The diagonal elements of the first three even-numbered waves, calculated from the Y. S. potential, are shown in figure 7. These partial waves were summed through $l = 4$ according to equation (D5b)), and then equations (13) were solved for the energy spectrum. Figure 8 gives the result. Curves obtained using only one or two partial waves in the reaction matrix are also shown. A comparison of the calculated spectrum with the experimentally measured one shows the energy scale of the present results to be nearly an order of magnitude too high.

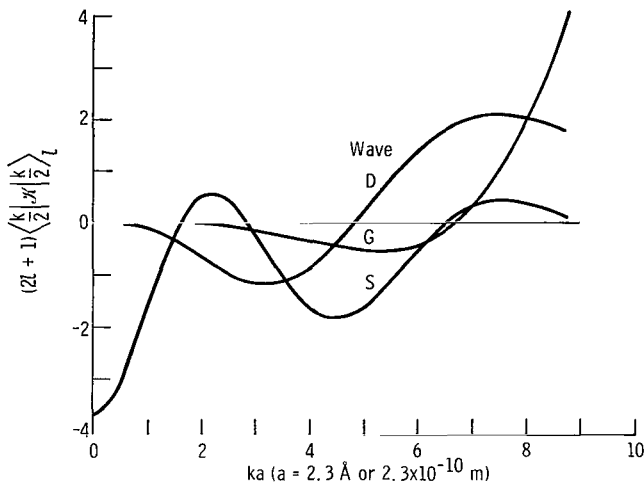


Figure 7. - Partial wave contributions to diagonal elements of reaction matrix for Yntema-Schneider potential.

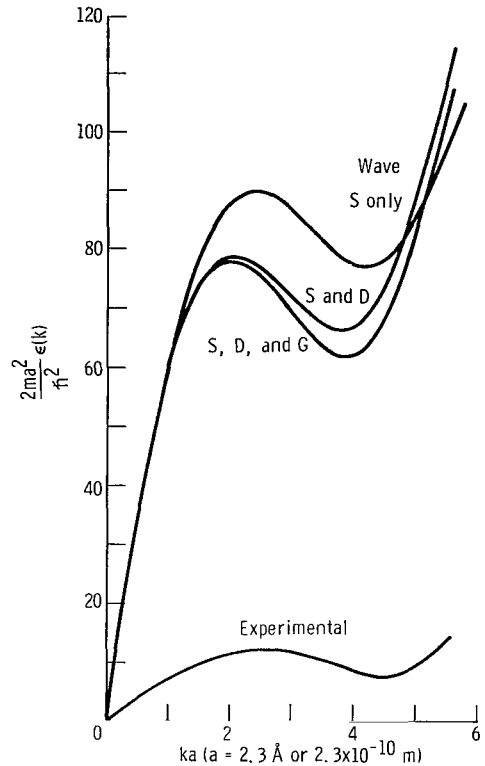


Figure 8. - Energy spectrum for Yntema-Schneider potential.

The disparity in scale tends to obscure the important similarities: the phonon-like low-momentum excitations and the roton minimum. The momenta at which the roton minimum and the relative maximum occur are approximately the same as those of the experimental spectrum. Previous attempts to include both singular core and attractive well have failed to reproduce even these qualitative features. Brueckner and Sawada's treatment (refs. 12 and 13) of the hard core gave a qualitatively good spectrum, and as noted in a previous section, gave semiquantitative agreement with the experimental spectrum for an appropriate choice of a parameter in the theory. But best agreement was achieved for a nonphysical value of the parameter that implied that the number of particles in excited states exceeded the total number of particles. The attempt by Parry and ter Haar to use Brueckner's method and to include an attractive well led to the loss of even the qualitative features of the helium II spectrum. In the context of these previous results, the qualitative features of the present spectrum - phonons at low momentum and roton minimum - are gratifying.

The speed of ordinary sound (first sound) is equal to the initial slope of the energy versus momentum curve, because for low-momentum phonons $\epsilon = pc$ where c is the speed of sound. The plot in figure 8 is of $E = 2ma^2\epsilon/\hbar^2$ as a function of ka where k is

the wave number and a is a reference dimension, taken here to be 2.3 \AA ($2.3 \times 10^{-10} \text{ m}$). In terms of the slope $dE/d(ka)$, evaluated at the origin,

$$c = \frac{d\epsilon}{dp} = \frac{\hbar^2}{2ma^2} \frac{a}{\hbar} \frac{dE}{d(ka)} = \frac{\hbar}{2ma} \frac{dE}{d(ka)}$$

The value of c from the Y. S. potential is 2300 meters per second, to be compared with the actual value of 240 meters per second extrapolated to $T = 0$.

It is easy to see what causes the integral equations for $E(ka)$ to give such high energies. It is primarily the influence of \mathcal{X}_{00} in the equations for $F(x)$ and $H(x)$. \mathcal{X}_{00} is a rather large negative number for the Y. S. potential because that potential is nearly attractive enough to produce a zero-energy bound state. A potential that is just strong enough to have a zero-energy bound state will have a scattering length of $-\infty$; and by appendix F, \mathcal{X}_{00} will also be $-\infty$. For large negative values of \mathcal{X}_{00} , the integrals in equations (13) may be neglected and the equations become approximately

$$F(x) = x^2 + 8\pi P_0 \left(\frac{2\mathcal{X}_{\frac{x}{2} \frac{x}{2}}}{2} - 3\mathcal{X}_{00} \right)$$

$$H(x) = 8\pi P_0 \mathcal{X}_{0x}$$

$$E(x) = \sqrt{F^2(x) - H^2(x)}$$

Near $x = 0$, $\mathcal{X}_{\frac{x}{2} \frac{x}{2}}$ and \mathcal{X}_{0x} have the following expansions:

$$\mathcal{X}_{\frac{x}{2} \frac{x}{2}} = \mathcal{X}_{00} + dx^2$$

$$\mathcal{X}_{0x} = \mathcal{X}_{00} + bx^2$$

Hence

$$E(ka) = \sqrt{(F + H)(F - H)}$$

$$= \sqrt{-128\pi^2 P_0^2 (2d + b) \mathcal{X}_{00}} ka$$

for small ka . The initial slope of the spectrum is thus approximately proportional to $\sqrt{-\mathcal{X}_{00}}$. But study of figure 9 shows the value of d increases rapidly as \mathcal{X}_{00} decreases. (The same is true for b .) Thus the initial slope of the spectrum is very roughly proportional to $-\mathcal{X}_{00}$, for large negative \mathcal{X}_{00} .

Figure 9 shows the extreme sensitivity of \mathcal{X}_{00} to the strength of the attractive well. The curves in that figure correspond to the potentials of figure 10. These potentials are identical in the core region but have potential wells of three different strengths. The two potentials with reduced well strength were obtained from the Y. S. potential by multiplying all negative values of $v(r)$ by a parameter α , having values of 0.8 and 0.6. The reduction of well strength to 60 percent of the Y. S. strength reduces \mathcal{X}_{00} to about 1/40 of the value it has for the Y. S. potential as shown in figure 9. This strong sensitivity of \mathcal{X}_{00} to well strength is what prompted the construction of the weakened-well potential of figure 4. This potential was designed to have a much smaller \mathcal{X}_{00} than that of Y. S. and yet to fit the measured second virial coefficients just as well.

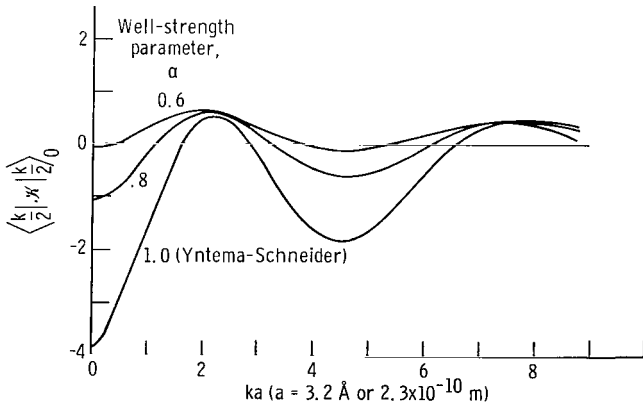


Figure 9. - Dependence of diagonal elements of K-matrix on well depth (S-wave only). Well-strength parameter α is defined by $v(r) = \alpha v_{YS}(r)$ for $v(r) < 0$.

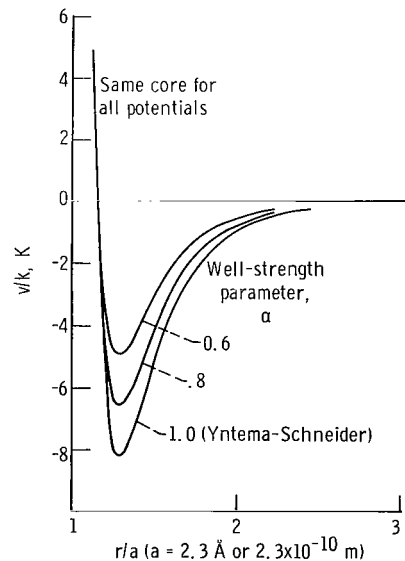


Figure 10. - Potentials with uniformly reduced wells. Potentials are identical for $v(r) > 0$. For $v(r) < 0$, potentials obey $v(r) = \alpha v_{YS}(r)$.

The weakened-well potential gives much better results than the Y. S. potential. Figure 11 shows the first three even partial waves of the diagonal elements of the reaction matrix. Comparison with figure 7 shows that \mathcal{X}_{00} is reduced to one-sixth of the Y. S. value. The consequent improvement in the energy scale of the spectrum is evident in figure 12. The improvement is significant but short of what is needed to agree with experiment. Comparing the spectrum with that of the Y. S. potential reveals a shift toward lower momentum of the roton minimum and of the relative maximum. The minimum is less pronounced. The fraction of particles in the condensed group of states is 91 percent, down slightly from the 93 percent result for the Y. S. potential.

There is some possibility that effects not taken into account in this work might lead to an effective weakening of the potential well. For example, the Hamiltonian upon which this work is based includes only two-body interaction terms. It is recognized that nonadditive three- and many-body interactions (refs. 38 and 39) exist in liquids because of the composite nature of the atoms. That is, because atoms are not simple "particles" but instead have internal structures and because the interparticle force is a result of a mod-

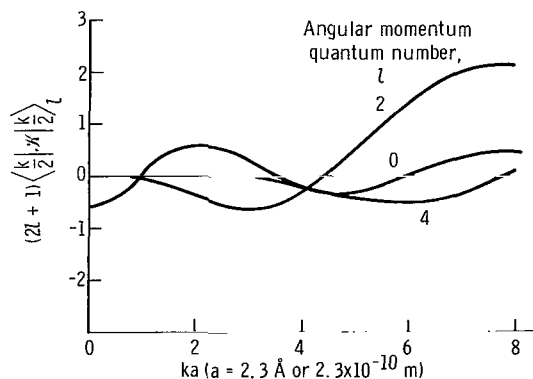


Figure 11. - Diagonal elements of reaction matrix for weakened-well potential.

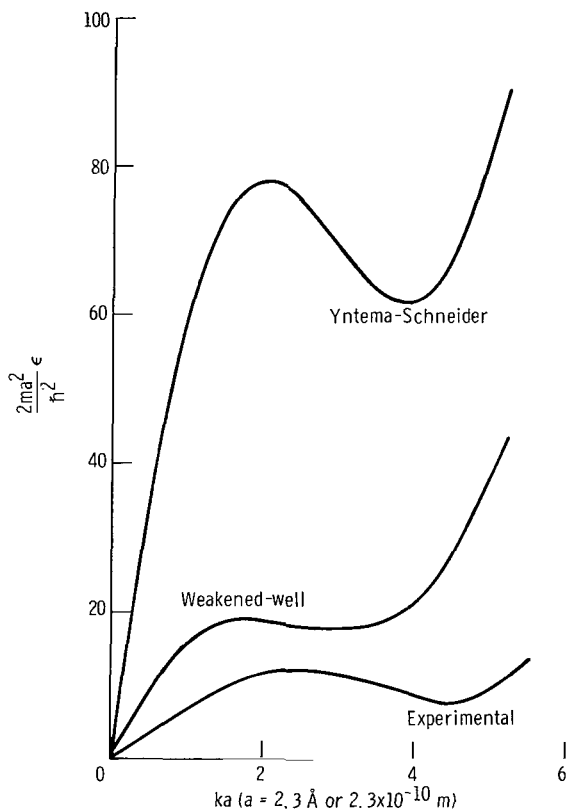


Figure 12. - Comparison of spectra from Yntema-Schneider and weakened-well potentials with experimental spectrum.

ification (polarization) of that structure, the force between a pair of atoms is not independent of the presence or absence of other atoms in the vicinity. At low densities this is unimportant. But at liquid helium density the effects may not be negligible. Inclusion of many-body interactions in the Hamiltonian⁵ is out of the question in the present theory, but it might be possible to include the many-particle effects approximately by modifying the two-particle potential to make it an "effective two-particle potential" appropriate for the observed liquid density. Whether the presence of the other particles weakens or strengthens the Van der Waals attraction between two particles is not at all obvious.

An approximate microscopic treatment of this problem (ref. 39), which yields a very small weakening of the attraction, is discussed in appendix G. Macroscopic methods tak-

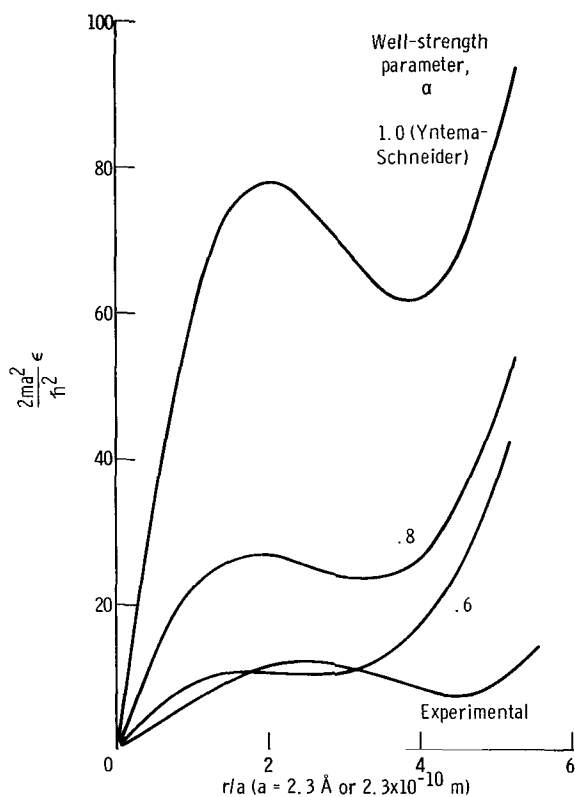


Figure 13. - Comparison of spectra for reduced wells. Well-strength parameter α is defined by $v(r) = \alpha v_S(r)$ for $v(r) \approx 0$.

⁵The distinction between the many-particle interactions under discussion here and "many-body terms" in a perturbation expansion must not be forgotten. Even if one could exactly diagonalize the Hamiltonian (eq. (2)), one would have in no way included many-particle interactions since equation (2) included only two-particle interactions.

ing frequency dependence of the dielectric constant into account (ref. 40) have not been applied to this specific problem. In any case, because many-body forces or some other phenomenon might effectively weaken the attractive well, it is desirable to calculate spectra for a series of wells of varying strength. Such an approach serves to uncover trends in the spectra and to further show the sensitivity to well strength.

The potentials of figure 10 form a series of three such potentials, related by the single parameter α . The calculated energy spectra can be compared in figure 13. The results show that as α decreases the energy scale of the spectrum improves and can even fall partially below the observed spectrum. A severe shift toward lower momentum occurs, however, which was noted in lesser degree in figure 12. The cause of this shift is not known.

DISCUSSION

Relation to Previous Work

To place the results in proper context, the following comparisons of the present methods and results are made with other work.

Most of the microscopic theories have been forced to deal with truncated Hamiltonians. Of these theories several are valid only for weak potentials. Bogoliubov (ref. 10) first obtained a phonon-like low-momentum spectrum for weak repulsive interactions near absolute zero. His Hamiltonian contained forward, exchange, and pair scattering terms, but was diagonalized only by approximating some of the operators by c-numbers. Wentzel (ref. 14) and Luban (ref. 15) found an energy gap at low momenta using the pair Hamiltonian. The helium II spectrum, of course, has no such gap. Using the idea of Girardeau (refs. 22 and 23) that, for an attractive interaction, condensation should occur into many states instead of into just one. Luban showed that the spectrum is phonon-like at low momentum for an appropriate attractive potential with pair scattering in the Hamiltonian. Hence the present work has assumed a generalized condensation and has included pair-to-pair scattering. The spectrum obtained herein has a phonon-like low-momentum region as observed in liquid helium II.

The aforementioned works by other authors were based on weak potentials. Brueckner and Sawada (refs. 12 and 13) used the reaction matrix method of handling strong potentials, but included only forward and exchange scattering and one special type of pair scattering in their Hamiltonian. For hard spheres with no attractive well, they found a phonon-like low-momentum spectrum. This is similar to Wentzel's result for repulsive but weak potentials. The Brueckner and Sawada spectrum had a roton minimum which approximated the experimental one for an appropriate choice of a parameter

in their theory. But this parameter was proportional to the density of condensed (zero-momentum) particles, and thus was not really arbitrary. In fact the value of the parameter giving the best spectrum leads to the contradiction that the density of excited particles is 2.7 times the total density. Parry and ter Haar (ref. 17) used approximately the same method but consistently handled the density of condensed particles. Their attempt to include an attractive well in the potential was unsuccessful. All qualitative similarity to the experimental spectrum was lost, including the phonon-like part.

The present work has used a reaction matrix to handle the strong repulsion. It differs from the Brueckner and Sawada reaction matrix, however, in that only kinetic energy is included in the propagator G . The additional terms included in the unperturbed Hamiltonian by Brueckner and Sawada and by Parry and ter Haar are not necessary with net attractive forces. The successful inclusion of the attractive potential in this work is due to including pair interaction terms and to assuming the generalized condensation.

The most significant result of this work is that the two important qualitative features of the helium potential - strong repulsion, but net attraction - have been treated with methods that were able to produce the two important qualitative features of the excitation spectrum - phonons and rotons.

Discussion of Approximations

As in all other attempts to derive the energy spectrum, simplifications and approximations have been made to make the problem tractable. The methods of this work have produced an energy spectrum of correct qualitative character from a microscopic theory using realistic potentials with both singular core and attractive well. It is appropriate to recapitulate the simplifications, approximations, and omissions since they may be responsible for the lack of quantitative agreement with experiment. Unfortunately the most important cause of error has not been identified because of the complexity of the integral equations.

The first simplification was to restrict the second-quantized Hamiltonian to two-body interaction terms. Three-, four-, and many-body operators have been omitted, but they should be included for an exact treatment of helium. It was shown in a previous section that a weakening of the attractive part of the potential by about 40 percent gives approximately the right speed of sound. Perhaps the interaction of two helium atoms could be modified to this degree by the presence of several near neighbors (speaking microscopically) or (speaking phenomenologically) by the presence of the dielectric medium composed of the other atoms. One treatment of many-body forces, cited in appendix G, gives only a 1 percent effect; however, it may not be accurate for liquid helium.

The second simplification was to truncate the Hamiltonian. Only forward scattering, exchange scattering, and pair scattering terms were retained. Ways of handling more terms than these are not known. Actually the use of K in place of V does, in effect, include more terms, but the form of the Hamiltonian is unchanged.

To allow the inclusion of a singular repulsive core in the potential, the V matrix elements were replaced by reaction matrix elements. This, in effect, presumed enough terms of the many-body perturbation series to give finite matrix elements in the interaction part of the Hamiltonian. But it is shown in appendix B that the perturbation series for the free energy derived from the "Hamiltonian" with K contains some duplicated terms. The extra terms needed to treat singular cores therefore came at the price of including some terms twice. This was recognized by previous authors (refs. 12, 13, and 17) but neglected on the basis of canceling errors for ground and excited states. But it cannot be said that the elementary excitation spectrum would be unaffected. The duplication of terms in the perturbation series for the free energy means the partition function would also be in error since

$$F = -kT \log Z$$

The justification for putting K into the Hamiltonian was valid only near absolute zero. This is, however, simply a limit on the allowed temperature rather than an approximation. If the method is used for elevated temperatures, then an approximation is thereby made.

The Wentzel TEH method is not an approximate method in itself. The equivalent Hamiltonian has exactly the same partition function as the Hamiltonian from which it was derived and thus the same thermodynamics. It has been argued in an earlier section that the spectrum of elementary excitations is also the same if it turns out to be temperature independent.

The last approximation made was to replace the two-body reaction matrix elements with their approximately equal one-body central-force counterparts. There is no reason, in principle, why this must be done. However, the solution of the integral equation for the one-body K matrix was barely practical. The numerical solution of the integral equation for a two-body K , which would be a function of four variables instead of two, would be impossible without completely different techniques.

The assumed generalized or "smeared" Bose-Einstein condensation is probably not an approximation. It has been shown (refs. 22, 23, and 28) to be a consequence of a predominantly attractive interaction, which permits the system to lower its energy by spreading out the condensate over many zero-energy (degenerate) but distinguishable states.

SUMMARY OF RESULTS

The central result of this work is that the qualitative features of the helium excitation spectrum have been derived microscopically from an interparticle potential containing a strong repulsive core and an attractive well. The strong repulsive core was handled by using reaction matrix elements instead of interparticle potential matrix elements in the Hamiltonian. The attractive well, which is strong enough in helium to give the potential a negative scattering length, was successfully included by assuming that a smeared Bose-Einstein condensation occurs. The pair Hamiltonian (which includes forward, exchange, and pair scattering interaction terms) was, in effect, diagonalized by the Thermodynamically Equivalent Hamiltonian method. The equations derived from these methods were solved numerically and yielded spectra with linear behavior at low momenta and roton regions at high momenta. These correct qualitative features have not previously been derived from a realistic interparticle potential, containing both a repulsive core and an attractive well. For the Yntema-Schneider potential for helium the calculated spectrum is in poor quantitative agreement with experiment. Weaker potential wells were shown to improve the energy scale of the spectrum substantially. A potential was exhibited which fits second virial coefficients as well as the Yntema-Schneider potential does, but which gave a much improved energy scale. Spectra calculated for a series of three potential wells of decreasing strengths showed improving energy scale but a shifting of the roton minimum toward lower momentum.

Lewis Research Center,
National Aeronautics and Space Administration,
Cleveland, Ohio, April 30, 1968,
129-02-05-16-22.

APPENDIX A

SYMBOLS

a	reference dimension, chosen herein as approximate core size: 2.3 \AA ($2.3 \times 10^{-10} \text{ m}$)	H_1	that part of H_p that does not contribute to thermodynamics
a_k^+, a_k	creation and annihilation operators for plane-wave states with wave vector \vec{k}	H'	perturbation Hamiltonian
B_k^+, B_k	auxiliary operators used in finding TEH	h_k	auxiliary function in integral equation for spectrum
B(T)	second virial coefficient	\hbar	Planck's constant/ 2π
C_k^+, C_k	auxiliary operators used in finding TEH	K	reaction matrix or operator
c	speed of first (ordinary) sound	\mathcal{K}	dimensionless reaction matrix, $K \times 2m\Omega/8\pi\hbar^2 a$
E(k)	with argument k: energy of state with wave number k	k	wave number; wave vector with vector sign deleted for simplicity
E(x)	with argument x or y: dimensionless energy $E(x) = \epsilon_k \times 2ma^2/\hbar^2$	l	angular momentum quantum number
F	Helmholtz free energy	M_n	n^{th} semiinvariant
F_0	Helmholtz free energy for non-interacting particles	m	mass of helium atom (or other boson)
f_k	auxiliary function in integral equations for spectrum	N	number of particles in system
G	Green's function	N_0	number of particles in the condensate
H	general second-quantized Hamiltonian including two-body interactions	n_0	Avogadro's number
H_0	unperturbed Hamiltonian	P	number of particles in cube of side a, $P = Na^3/\Omega$
H_p	pair Hamiltonian	P_0	number of condensed particles in cube of side a, $P_0 = N_0 a^3/\Omega$
H_{TE}	thermodynamically equivalent Hamiltonian	p	(without subscript) momentum
		p'	momentum at which roton minimum occurs

p_i	wave number; sometimes momentum	x	dimensionless wave number, $x = ka$
p_0	nonzero wave number below which smeared condensate forms	Z	canonical partition function
\mathcal{Q}	grand partition function	α	well-strength parameter, $\alpha = 1.0$ for Y.S. potential
r	radial coordinate in spherical coordinate system	β	$1/kT$ where k is Boltzmann's constant
T	absolute temperature	γ	r/a
U	c-number appearing in TEH	ϵ_k	energy of elementary excitation with wave number k
U_0	c-number appearing in TEH	η_k	variational parameter, finally set equal to $\langle a_{-k}^+ a_k^+ \rangle$
V	two-particle interaction potential energy operator; one-particle potential energy operator	μ	chemical potential
V_0	potential inside strong uniform repulsive core	ξ_k	variational parameter, finally set equal to $\langle a_k^+ a_k \rangle$
$\mathcal{V}(\gamma)$	$v(r) \times ma^2/\hbar^2$	ρ	density, N/Ω
$v(r)$	spherically symmetric interaction potential energy function	Ω	volume of system
$\hat{v}(q)$	three-dimensional Fourier transform of $v(r)$ divided by Ω , for momentum transfer q	ω_k	energy of free particle with wave number k

APPENDIX B

USE OF K INSTEAD OF V

Consider the expansion of the free energy F in a series of "semiinvariants." (See for example, refs. 41 and 42.) Let the exact nontruncated Hamiltonian be split into the unperturbed part H_0 (kinetic energy) and the perturbation H' (interaction terms), that is,

$$H = H_0 + H'$$

Then $F - F_0 = \sum_{n=1}^{\infty} M_n/n!$ where F_0 is the unperturbed free energy and

$$M_1 = \frac{1}{\beta} \int_0^\beta \langle H'(\lambda) \rangle d\lambda$$

$$M_2 = \frac{1}{\beta} \int_0^\beta d\lambda \int_0^\lambda d\lambda' [\langle H'(\lambda)H'(\lambda') \rangle - \langle H'(\lambda) \rangle \langle H'(\lambda') \rangle]$$

$$M_3 = \frac{1}{\beta} \int_0^\beta d\lambda \int_0^\lambda d\lambda' \int_0^{\lambda'} d\lambda'' [\langle H'(\lambda)H'(\lambda')H'(\lambda'') \rangle - 3\langle H'(\lambda)H'(\lambda') \rangle \langle H'(\lambda'') \rangle + 2\langle H'(\lambda) \rangle \langle H'(\lambda') \rangle \langle H'(\lambda'') \rangle]$$

The bracket means thermodynamic expectation value and is defined as follows:

$$\langle \theta \rangle \equiv \frac{\text{tr} \left(\theta e^{-\beta H_0} \right)}{\text{tr} \left(e^{-\beta H_0} \right)}$$

where "tr" may be taken to mean a sum over all sets of occupation numbers of the eigenstates of H_0 . $H'(\lambda)$ is a temperature analogue of the interaction picture of an operator. Its definition is

$$H'(\lambda) \equiv e^{\lambda H_0} H' e^{-\lambda H_0}$$

The operator H' for a complete (nontruncated) second-quantized Hamiltonian including only two-body interactions⁶ is

$$H' = \frac{1}{2} \sum_{k_1 k_2 k_3 k_4} \langle k_1 k_2 | V | k_3 k_4 \rangle a_{k_1}^+ a_{k_2}^+ a_{k_3} a_{k_4} \quad (B1)$$

as in equation (2). The a^+ 's and a 's, respectively, create and annihilate plane-wave states with the indicated wave vectors.

The expectation values $\langle \theta \rangle$ are exceedingly complicated for $T \neq 0$ (finite β). Also the replacement of V by K in the Hamiltonian is valid only at or very near zero temperature. Therefore, only the limit of zero temperature ($\beta = (1/kT) \rightarrow \infty$) is considered in this work. The excitation spectrum, which is the primary result of this work, is thus valid only near $T = 0$. The use here of the TEH method of Wentzel, is justified, and in fact the meaning of "excitation spectrum" is definite, only if the spectrum is temperature independent for a range of temperature near $T = 0$. These points are discussed in the body of this report.

At arbitrary temperature

$$\langle \theta \rangle = \frac{\sum_{\{n_i\}} \langle n_0, n_1, n_2, \dots | \theta e^{-\beta H_0} | n_0, n_1, n_2, \dots \rangle}{\sum_{\{n_i\}} \langle n_0, n_1, n_2, \dots | e^{-\beta H_0} | n_0, n_1, n_2, \dots \rangle}$$

where $\sum_{\{n_i\}}$ indicates a sum over all possible sets of n_0, n_1, n_2, \dots , and

$i = 0, 1, 2, \dots$ indicate various free-particle states, that is, eigenstates of H_0 , the kinetic energy. The zero subscript here indicates the zero-momentum state. As $T \rightarrow 0$ and hence $\beta \rightarrow \infty$ the factor $e^{-\beta H_0}$ in the numerator causes all other terms to become negligible compared to the ground state term, $n_0 = N$ and $n_i = 0$ for $i > 0$. Thus

⁶Note there is a clear distinction between two-body interactions and two-, three-, or n-body terms in a perturbation expansion.

$$\lim_{T \rightarrow 0} \langle \mathcal{O} \rangle = \lim_{\beta \rightarrow \infty} \langle \mathcal{O} \rangle = \frac{\langle N, 0, 0, \dots | \mathcal{O} | N, 0, 0, \dots \rangle}{\langle N, 0, 0, \dots | 1 | N, 0, 0, \dots \rangle} = \langle 0 | \mathcal{O} | 0 \rangle$$

where $|0\rangle \equiv |N, 0, 0, 0, \dots\rangle$ denotes the ground state of a system of noninteracting bosons, which is all particles in the zero-momentum state.

The first few semiinvariants can now be evaluated in the zero-temperature limit

$$\begin{aligned} M_1 &= \frac{1}{\beta} \left\langle \int_0^\beta H'(\lambda) d\lambda \right\rangle \rightarrow \lim_{\beta \rightarrow \infty} \frac{1}{\beta} \int_0^\beta \langle H'(\lambda) \rangle d\lambda \\ &= \lim_{\beta \rightarrow \infty} \frac{1}{\beta} \int_0^\beta d\lambda \langle 0 | H'(\lambda) | 0 \rangle \\ &= \lim_{\beta \rightarrow \infty} \frac{1}{\beta} \int_0^\beta d\lambda \langle 0 | e^{\lambda H_0} H' e^{-\lambda H_0} | 0 \rangle \\ &= \frac{1}{2} \lim_{\beta \rightarrow \infty} \frac{1}{\beta} \sum_{k_1 k_2 k_3 k_4} \int_0^\beta d\lambda \langle 0 | e^{\lambda H_0} a_{k_1}^+ a_{k_2}^+ a_{k_3} a_{k_4} e^{-\lambda H_0} | 0 \rangle \langle k_1 k_2 | V | k_3 k_4 \rangle \\ &= \frac{1}{2} \lim_{\beta \rightarrow \infty} \frac{1}{\beta} \sum_{k_1 k_2 k_3 k_4} \int_0^\beta d\lambda \langle 0 | e^{\lambda(\omega_{k_1} + \omega_{k_2} - \omega_{k_3} - \omega_{k_4})} a_{k_1}^+ a_{k_2}^+ a_{k_3} a_{k_4} | 0 \rangle \langle k_1 k_2 | V | k_3 k_4 \rangle \end{aligned}$$

Here ω_{k_i} is the kinetic energy of a particle with wave number k_i . But

$\langle 0 | a_{k_1}^+ a_{k_2}^+ a_{k_3} a_{k_4} | 0 \rangle = 0$ except for $k_1 = k_2 = k_3 = k_4 = 0$. Further $\omega_0 = 0$ and

$\langle 0 | a_0^+ a_0^+ a_0 a_0 | 0 \rangle = \langle 0 | a_0^+(a_0 a_0^+ - 1)a_0 | 0 \rangle = N_0^2 - N_0 = N^2 - N \approx N^2$ for N large. Then

$$\lim_{\beta \rightarrow \infty} M_1 = \frac{1}{2} \lim_{\beta \rightarrow \infty} \frac{1}{\beta} \int_0^\beta d\lambda N^2 \langle 0 | V | 0 \rangle = \frac{1}{2} \rho N \hat{v}(0) \quad (\text{B2})$$

where $\hat{v}(0)/\Omega = \langle 0|V|0\rangle$. The second semiinvariant becomes, as $\beta \rightarrow \infty$

$$\begin{aligned}
\lim_{\beta \rightarrow \infty} M_2 &= -\lim_{\beta \rightarrow \infty} \frac{1}{\beta} \int_0^\beta d\lambda \int_0^\lambda d\lambda' [\langle H'(\lambda)H'(\lambda') \rangle - \langle H'(\lambda) \rangle \langle H'(\lambda') \rangle] \\
&= -\frac{1}{4} \lim_{\beta \rightarrow \infty} \frac{1}{\beta} \int_0^\beta d\lambda \int_0^\lambda d\lambda' \sum_{\substack{k_1 k_2 k_3 k_4 \\ k_5 k_6 k_7 k_8}} \langle k_1 k_2 | V | k_3 k_4 \rangle \langle k_5 k_6 | V | k_7 k_8 \rangle \\
&\quad \times e^{\lambda(\omega_{k_1} + \omega_{k_2} - \omega_{k_3} - \omega_{k_4})} e^{\lambda'(\omega_{k_5} + \omega_{k_6} - \omega_{k_7} - \omega_{k_8})} \\
&\quad \times \left[\langle 0 | a_{k_1}^+ a_{k_2}^+ a_{k_3} a_{k_4} a_{k_5}^+ a_{k_6}^+ a_{k_7} a_{k_8} | 0 \rangle - \langle 0 | a_{k_1}^+ a_{k_2}^+ a_{k_3} a_{k_4} | 0 \rangle \langle 0 | a_{k_5}^+ a_{k_7}^+ a_{k_8} a_{k_9} | 0 \rangle \right] \\
&= -\frac{1}{4} \lim_{\beta \rightarrow \infty} \frac{1}{\beta} \int_0^\beta d\lambda \int_0^\lambda d\lambda' \left[\sum_{k_3 k_4 k_5 k_6} \langle 00 | V | k_3 k_4 \rangle \langle k_5 k_6 | V | 00 \rangle \right. \\
&\quad \times e^{-\lambda(\omega_{k_3} + \omega_{k_4}) + \lambda'(\omega_{k_5} + \omega_{k_6})} \\
&\quad \left. \times \langle 0 | a_0^+ a_0^+ a_{k_3} a_{k_4} a_{k_5}^+ a_{k_6}^+ a_0 a_0 | 0 \rangle - \langle 00 | V | 00 \rangle^2 \langle 0 | a_0^+ a_0^+ a_0 a_0 | 0 \rangle^2 \right]
\end{aligned}$$

where only $k_1 = k_2 = k_7 = k_8 = 0$ appear since other terms have zero expectation value in the noninteracting ground state. Only those elements of the V matrix which conserve total momentum give nonzero contributions, so

$$\begin{aligned}
\lim_{\beta \rightarrow \infty} M_2 &= -\frac{1}{4} \lim_{\beta \rightarrow \infty} \frac{1}{\beta} \int_0^\beta d\lambda \int_0^\lambda d\lambda' \left[2 \sum_{\mathbf{k} \neq 0} \frac{\hat{v}^2(\mathbf{k})}{\Omega^2} e^{-2\lambda\omega_{\mathbf{k}} + 2\lambda'\omega_{\mathbf{k}}} \right. \\
&\quad \times \langle 0 | a_0^\dagger a_0^\dagger a_{-\mathbf{k}} a_{\mathbf{k}} a_{-\mathbf{k}}^\dagger a_{\mathbf{k}}^\dagger a_0 a_0 | 0 \rangle + \frac{\hat{v}^2(0)}{\Omega^2} \langle 0 | a_0^\dagger a_0^\dagger a_0 a_0 a_0^\dagger a_0^\dagger a_0 a_0 | 0 \rangle - \frac{\hat{v}^2(0)}{\Omega^2} N^2 (N-1)^2 \left. \right] \\
&= -\frac{1}{4} \lim_{\beta \rightarrow \infty} \frac{1}{\beta} \int_0^\beta d\lambda \int_0^\lambda d\lambda' \left[\frac{2}{\Omega^2} \sum_{\mathbf{k} \neq 0} \hat{v}^2(\mathbf{k}) e^{-\lambda \hbar^2 \mathbf{k}^2 / m + \lambda' \hbar^2 \mathbf{k}^2 / m} N(N-1) \right] \\
&= -\frac{1}{2} \frac{\rho(N-1)}{\Omega} \lim_{\beta \rightarrow \infty} \frac{1}{\beta} \sum_{\mathbf{k} \neq 0} \hat{v}^2(\mathbf{k}) \int_0^\beta d\lambda e^{-\lambda \hbar^2 \mathbf{k}^2 / m} \left(\frac{e^{\lambda \hbar^2 \mathbf{k}^2 / m} - 1}{\hbar^2 \mathbf{k}^2 / m} \right) \\
&= -\frac{\rho N}{2\Omega} \lim_{\beta \rightarrow \infty} \frac{1}{\beta} \sum_{\mathbf{k} \neq 0} \frac{m \hat{v}^2(\mathbf{k})}{\hbar^2 \mathbf{k}^2} \left(\beta + \frac{e^{-\beta \hbar^2 \mathbf{k}^2 / m} - 1}{\hbar^2 \mathbf{k}^2 / m} \right) \\
&= -\frac{\rho N}{2} \frac{1}{8\pi^3} \int d^3 \mathbf{k} \frac{m \hat{v}^2(\mathbf{k})}{\hbar^2 \mathbf{k}^2} \\
&= -\frac{\rho N}{2} \frac{1}{2\pi^2} \frac{m}{\hbar^2} \int_0^\infty \hat{v}^2(k) dk \tag{B3}
\end{aligned}$$

In appendix H it is shown that

$$\begin{aligned} \lim_{\beta \rightarrow \infty} M_3 = & \frac{\rho N}{8} \frac{1}{(2\pi)^6} \frac{m^2}{\hbar^4} \int d^3 k_1 \int d^3 k_2 \frac{\hat{v}(k_1)}{k_1^2} \frac{\hat{v}(k_2)}{k_2^2} \hat{v}(k_1 - k_2) \\ & + \frac{\rho^2 N}{8} \frac{1}{(2\pi)^3} \frac{m^2}{\hbar^4} \hat{v}(0) \int d^3 k \frac{\hat{v}^2(k)}{k^4} \quad (\text{B4}) \end{aligned}$$

The first three terms in the expansion of the free energy of a nontruncated Hamiltonian are sufficient to indicate what type of "reaction" matrix may be used in the truncated Hamiltonian H_p to introduce more terms into the expansion.

Consider first the series expansion of a general element of the reaction matrix with respect to two-particle (noninteracting) plane-wave states

$$\begin{aligned} \langle k_1 k_2 | K | k_3 k_4 \rangle &= \langle k_1 k_2 | (V + VGV + VGVGV + \dots) | k_3 k_4 \rangle \\ &= \langle k_1 k_2 | V | k_3 k_4 \rangle + \sum_{k_5 k_6 k_7 k_8} \langle k_1 k_2 | V | k_5 k_6 \rangle \langle k_5 k_6 | G | k_7 k_8 \rangle \langle k_7 k_8 | V | k_3 k_4 \rangle \\ &\quad + \sum_{\substack{k_5 k_6 k_7 k_8 \\ k_9 k_{10} k_{11} k_{12}}} \langle k_1 k_2 | V | k_5 k_6 \rangle \langle k_5 k_6 | G | k_7 k_8 \rangle \langle k_7 k_8 | V | k_9 k_{10} \rangle \\ &\quad \times \langle k_9 k_{10} | G | k_{11} k_{12} \rangle \langle k_{11} k_{12} | V | k_3 k_4 \rangle + \dots \quad (\text{B5}) \end{aligned}$$

Many of the terms vanish because V has nonzero elements only between momentum-conserving states.

The plan is to insert the elements of K into the truncated Hamiltonian (eq. (3)) in place of the corresponding elements of V . If the free energy is now expanded in a perturbation series with K 's instead of V 's in the interaction term of H_p , the series will contain in first order many terms which previously appeared in higher order. Each higher order of the series with K in the truncated Hamiltonian has terms which the se-

ries with V had only in higher orders or not at all. It is therefore hoped that the series based on K (in the truncated Hamiltonian) more nearly resembles the exact perturbation series based on a nontruncated Hamiltonian. This can be achieved if G is chosen so its matrix elements contain the same energy denominators as those which appear in the exact perturbation series. The first semiinvariant containing K in place of V will now be examined to show what G must be chosen. It will be seen that "zero-energy" propagators should be used.

Clearly the first term in the expansion (eq. (B5)), which is simply the potential itself, will make the same contribution to the free energy as the potential would have made. Consider, however, the "second-order" terms of equation (B5),

$$\sum_{k_5 k_6 k_7 k_8} \langle k_1 k_2 | V | k_5 k_6 \rangle \langle k_5 k_6 | G | k_7 k_8 \rangle \langle k_7 k_8 | V | k_3 k_4 \rangle, \text{ and their contribution to } M_1.$$

Note first that only $k_1 = k_2 = k_3 = k_4 = 0$ make any contribution at all to M_1 . Further, since momentum-nonconserving elements of V vanish, only terms with $k_5 = -k_6$ and $k_7 = -k_8$ appear. Further, where G is defined using H_0 as the kinetic energy alone, only terms with $k_5 = k_7$ will be nonzero. Hence the second-order terms in equation (B5) give in M_1 (as $\beta \rightarrow \infty$)

$$\begin{aligned} \frac{1}{2} N^2 \sum_{\mathbf{k}} \langle 00 | V | \mathbf{k} - \mathbf{k} \rangle \langle \mathbf{k} - \mathbf{k} | G | \mathbf{k} - \mathbf{k} \rangle \langle \mathbf{k} - \mathbf{k} | V | 00 \rangle &= \frac{1}{2} \rho \frac{N}{\Omega} \sum_{\mathbf{k}} \frac{\hat{v}^2(\mathbf{k})}{E - \hbar^2 \mathbf{k}^2 / m} \\ &= -\frac{\rho N}{2} \frac{1}{2\pi^2} \int_0^\infty \frac{k^2 v^2(k) dk}{-E + \hbar^2 k^2 / m} \quad (\text{B6}) \end{aligned}$$

This term has the same form as the second-order terms in the perturbation series based on V if E is set equal to zero. The resulting zero-energy propagator contains the same energy denominators which arise in M_2 upon integrating with respect to λ' (see algebra leading to eq. (B3)). In a similar way the third-order terms in equation (B5) produce terms in M_1 with the right type of energy denominators if E is always set equal to zero. This value for E was also used by Brueckner and Sawada (refs. 12 and 13).

A Green's function is not uniquely specified until the manner of handling the singularities is given. If the principal value is taken, then the solution of equation (4) is called the reaction matrix. If the integration follows a contour in the complex plane which goes above one singularity and below the other (for $E \neq 0$), then the solution of equation (4) is called the T matrix and may be either " T_+ " or " T_- ," depending on which of the two possible ways of going over and under are chosen. The principal value should be used because the integrals (such as eq. (B6)) which arise from the expansion of K in terms of V actually come from sums over intermediate states. These sums should be like those that occur in the semiinvariants M_i . The sums occurring there appeared first as the sums in the interaction parts of the Hamiltonian (eq. (B1)). There $\vec{k}_1, \vec{k}_2, \vec{k}_3,$ and \vec{k}_4 are the allowed wave vectors of plane waves. As the thermodynamic limit is taken, the equally spaced allowed values of x-, y-, and z-components of any \vec{k}_i become more and more closely spaced. The sum over the states (see eq. (B5)), second term) therefore approaches the principal value of the integral (by the definition of the latter).

As previously noted (refs. 12, 13, and 17), the use of a reaction matrix is seen to cause a duplication of some terms in the perturbation expansion. The "first-order" term of equation (B5), which is simply the potential, produces the result (eq. (B3)) in M_2 , that is,

$$-\frac{1}{2} \rho N \frac{1}{2\pi^2} \frac{1}{\hbar^2} \int_0^\infty m \hat{v}^2(k) dk$$

But the same contribution is produced by the second terms of equation (B5) in M_1 as shown in equation (B6). Similar duplications occur in higher order, though not every term is duplicated. According to Parry and ter Harr (ref. 17), it can be shown that, if the linked cluster expansion is valid, the same error occurs in the energy of an excited state as in the ground state energy. Therefore, the total energy of the system is expected to be incorrectly given by this model, but if a small amount of thermal excitation is allowed, the difference between the excited and ground state energies will not contain the error.

APPENDIX C

CALCULATION OF REACTION MATRIX ELEMENTS

The types of reaction matrix elements needed are

$$\left. \begin{aligned} &\langle p - p | K | p - p \rangle \\ &\langle p - p | K | -pp \rangle \\ &\langle kp | K | kp \rangle \\ &\langle kp | K | pk \rangle \end{aligned} \right\} \quad (C1)$$

(As usual the quantities k and p are vectors, but the vector symbol is suppressed for simplicity.) The required elements include those in which k or p may be zero. How these elements may be calculated will be discussed here. To reduce the calculation to manageable size in terms of machine memory storage and computing time, an approximation called the center-of-mass approximation is made. It reduces the elements (eq. (C1)) to elements of a one-particle K operator with respect to one-particle states.

The K matrix needed is defined by the integral equation

$$K = V + VGK = V + VGV + VGVGV + \dots$$

where V is the interparticle potential. G has been chosen in this work to be a zero-energy Green's function

$$G = \frac{1}{-H_0}$$

where H_0 is the unperturbed Hamiltonian, taken to be simply the kinetic energy alone.

The elements of K with respect to two-body free-particle states are required, that is,

$$\langle k_1 k_2 | K | k_3 k_4 \rangle$$

where $|k_3 k_4\rangle$ is a state with the wave function $(1/\Omega)e^{i\vec{k}_3 \cdot \vec{r}_1} e^{i\vec{k}_4 \cdot \vec{r}_2}$. A general element of the K matrix then satisfies the following equation:

$$\langle k_1 k_2 | K | k_3 k_4 \rangle = \langle k_1 k_2 | V | k_3 k_4 \rangle + \sum_{k_5 k_6 k_7 k_8} \langle k_1 k_2 | V | k_5 k_6 \rangle \langle k_5 k_6 | G | k_7 k_8 \rangle \langle k_7 k_8 | K | k_3 k_4 \rangle$$

The operator G is diagonal with respect to free-particle eigenfunctions because H_0 is diagonal. Thus,

$$\langle k_5 k_6 | G | k_7 k_8 \rangle = - \frac{\delta_{k_5 k_7} \delta_{k_6 k_8}}{H_0} = \frac{\delta_{k_5 k_7} \delta_{k_6 k_8}}{\hbar^2 (k_5^2 + k_6^2) / 2m} \quad (C2)$$

Hence

$$\langle k_1 k_2 | K | k_3 k_4 \rangle = \langle k_1 k_2 | V | k_3 k_4 \rangle - \sum_{k_5 k_6} \langle k_1 k_2 | V | k_5 k_6 \rangle \frac{2m/\hbar^2}{k_5^2 + k_6^2} \langle k_5 k_6 | K | k_3 k_4 \rangle$$

The V matrix elements may be reduced to one-body matrix elements of a single-particle central potential

$$\begin{aligned} \langle k_1 k_2 | V | k_3 k_4 \rangle &= \int d^3 r_1 d^3 r_2 \langle \vec{k}_1 \vec{k}_2 | \vec{r}_1 \vec{r}_2 \rangle \langle \vec{r}_1 \vec{r}_2 | V | \vec{r}_1 \vec{r}_2 \rangle \langle \vec{r}_1 \vec{r}_2 | \vec{r}_3 \vec{r}_4 \rangle \\ &= \frac{1}{\Omega^2} \int d^3 r_1 d^3 r_2 e^{i(\vec{k}_1 \cdot \vec{r}_1 + \vec{k}_2 \cdot \vec{r}_2 - \vec{k}_3 \cdot \vec{r}_1 - \vec{k}_4 \cdot \vec{r}_2)} v(\vec{r}_1 - \vec{r}_2) \\ &= \frac{1}{\Omega} \int d^3 r e^{i(\vec{k}_1 - \vec{k}_3) \cdot \vec{r}} v(r) \delta_{k_1 + k_2, k_3 + k_4} \end{aligned}$$

where $\vec{r} = \vec{r}_1 - \vec{r}_2$ and the expression has been integrated with respect to the center-of-mass coordinate \vec{R} . The central potential $v(r)$ has the following one-body matrix elements:

$$\begin{aligned}
\left\langle \frac{k_1 - k_2}{2} \left| V \right| \frac{k_3 - k_4}{2} \right\rangle &= \frac{1}{\Omega} \int d^3r e^{i\left(\frac{k_1 - k_2}{2} - \frac{k_3 - k_4}{2}\right) \cdot r} v(r) \\
&= \frac{1}{\Omega} \int d^3r e^{i\left(\frac{k_1 - k_3}{2} + \frac{k_1 - k_3}{2}\right) \cdot r} v(r) \quad \text{for } k_1 + k_2 = k_3 + k_4 \\
&= \frac{1}{\Omega} \int d^3r e^{i(k_1 - k_3) \cdot r} v(r)
\end{aligned}$$

This is the same as $\langle k_1 k_2 | V | k_3 k_4 \rangle$. The matrix elements of G , however, do not thus reduce to one-body elements. Let the definition of the center-of-mass (one-body) G be

$$G = \frac{1}{-H_0} = \frac{1}{-\hbar^2 k^2 / m}$$

where m occurs rather than $2m$ because the reduced mass is $m/2$. Matrix elements are taken with respect to single-particle plane-wave states. Then

$$\left\langle \frac{k_1 - k_2}{2} \left| G \right| \frac{k_3 - k_4}{2} \right\rangle = - \frac{\delta_{k_1 - k_2, k_3 - k_4}}{\hbar^2 (k_1 - k_2)^2 / 4m} = - \frac{\delta_{k_1 - k_2, k_3 - k_4}}{\hbar^2 (k_1^2 + k_2^2 - 2k_1 k_2) / 4m}$$

This quantity approaches the form of the two-body element (eq. (C2)) if $\vec{k}_1 \approx -\vec{k}_2$. It equals the two-body element for a pair excitation, where k_1 and k_2 are equal and opposite momenta, produced, for example, by pair-to-pair scattering from the condensate. For \vec{k}_1 and \vec{k}_2 such that the total momentum is not negligible compared to the relative momentum, the approximation is poorer. The exact effect of using this approximation is

certainly not known for the present application.⁷ Parry and ter Haar (ref. 17) made some approximate calculations to estimate errors and drew the qualitative conclusion that the error would be small.

The matrix elements (eqs. (C1)) thus reduce (to the accuracy of the center-of-mass approximation) as follows:

$$\langle p - p | K | p - p \rangle \rightarrow \langle p | K | p \rangle \equiv K_{pp}$$

$$\langle p - p | K | -pp \rangle \rightarrow \langle p | K | -p \rangle \equiv K_{p-p}$$

$$\langle kp | K | kp \rangle \rightarrow \left\langle \frac{k-p}{2} | K | \frac{k-p}{2} \right\rangle \equiv K_{\frac{k-p}{2} \frac{k-p}{2}}$$

$$\langle kp | K | pk \rangle \rightarrow \left\langle \frac{k-p}{2} | K | \frac{p-k}{2} \right\rangle \equiv K_{\frac{k-p}{2} \frac{p-k}{2}}$$

There are no special problems in calculating the first two of the elements. The elements $K_{\frac{k-p}{2} \pm \frac{k-p}{2}}$ are really of the simple form $K_{\vec{q} \pm \vec{q}}$ where $\vec{q} = (\vec{k} - \vec{p})/2$ (fig. 14). In the integral equations derived in the text, these elements appear in an integral of the form

$$\frac{\Omega}{(2\pi)^3} \int d^3p K_{\frac{\vec{k}-\vec{p}}{2} \frac{\vec{k}-\vec{p}}{2}} \xi(p)$$

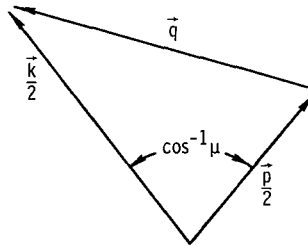


Figure 14. - Change of variables.

⁷It has been used in related treatments of the imperfect boson gas (refs. 12, 13, and 17).

Note that $q = \frac{1}{2} \sqrt{k^2 + p^2 - 2kp\mu}$ from the law of cosines, where μ is the cosine of the angle between \vec{k} and \vec{p} . Let the polar axis of the \vec{p} -space be parallel to \vec{k} , and denote $K_{\frac{k-p}{2} \pm \frac{k-p}{2}} = K_{q \pm q}$ by $K_{\pm}(q)$. Then

$$\begin{aligned}
 \frac{\Omega}{8\pi^3} \int d^3p K_{\frac{k-p}{2} \pm \frac{k-p}{2}} \xi(p) &= \frac{\Omega}{4\pi^2} \int_0^\infty p^2 dp \xi(p) \int_{-1}^1 d\mu K_{\pm} \left(\frac{1}{2} \sqrt{k^2 + p^2 - 2kp\mu} \right) \\
 &= \frac{\Omega}{\pi^2} \int_0^\infty p^2 dp \xi(p) \int_{q=|k-p|/2}^{q=(k+p)/2} dq \frac{q}{kp} K_{\pm}(q) \\
 &= \frac{\Omega}{\pi^2 k} \int_0^\infty p dp \xi(p) \int_{|k-p|/2}^{(k+p)/2} q K_{\pm}(q) dq \\
 &= \frac{\Omega}{\pi^2 k} \int_0^\infty p dp \xi(p) \left[Q_{\pm} \left(\frac{k+p}{2} \right) - Q_{\pm} \left(\frac{|k-p|}{2} \right) \right]
 \end{aligned}$$

where

$$Q_{\pm}(z) \equiv \int_0^z z' K_{\pm}(z') dz'$$

APPENDIX D

PARTIAL WAVE DECOMPOSITION OF REACTION MATRIX

As previously stated, the two-body reaction matrix elements will be approximated by the one-body, center-of-mass elements. The integral equation for that operator is

$$\mathbf{K} = \mathbf{V} + \mathbf{V}\mathbf{G}\mathbf{K}$$

where $\mathbf{G} = -1/H_0$. The desired matrix elements then satisfy the following equation:

$$\begin{aligned} \langle \vec{k} | \mathbf{K} | \vec{p} \rangle &= \langle \vec{k} | \mathbf{V} | \vec{p} \rangle + \langle \vec{k} | \mathbf{V}\mathbf{G}\mathbf{K} | \vec{p} \rangle \\ &= \langle \vec{k} | \mathbf{V} | \vec{p} \rangle + \frac{1}{(2\pi)^3} \int d^3q \langle \vec{k} | \mathbf{V} | \vec{q} \rangle \frac{-m\Omega}{\hbar^2 q^2} \langle \vec{q} | \mathbf{K} | \vec{p} \rangle \end{aligned} \quad (\text{D1})$$

The calculation is facilitated by decomposing the terms into angular momentum partial waves. Thus a matrix element of an operator \mathcal{O} may be written as

$$\langle \vec{k} | \mathcal{O} | \vec{p} \rangle \equiv \sum_l (2l + 1) \langle k | \mathcal{O} | p \rangle_l P_l(\hat{k} \cdot \hat{p})$$

where \hat{k} and \hat{p} are unit vectors parallel to \vec{k} and \vec{p} , respectively, $P_l(x)$ is a Legendre polynomial, and

$$\langle k | \mathcal{O} | p \rangle_l \equiv \frac{1}{2} \int_{-1}^1 \langle \vec{k} | \mathcal{O} | \vec{p} \rangle P_l(\hat{k} \cdot \hat{p}) d(\hat{k} \cdot \hat{p})$$

The Legendre polynomials have the property that

$$\int_{-1}^1 P_l(\mu) P_m(\mu) d\mu = \frac{2\delta_{lm}}{2l + 1}$$

Choosing a spherical coordinate system with \vec{k} parallel to the polar axis and with \vec{p} having an azimuthal angle of zero (see fig. 15), multiplying the terms in equation (D1)

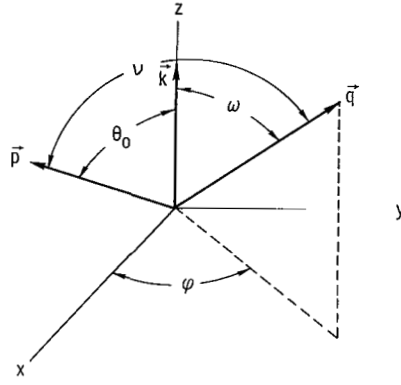


Figure 15. - Visual aid for partial wave expansion.

by $\frac{1}{2} P_l(\hat{\mathbf{k}} \cdot \hat{\mathbf{p}})$, and integrating over all values of $\hat{\mathbf{k}} \cdot \hat{\mathbf{p}}$ between -1 and 1 result in

$$\begin{aligned} \frac{1}{2} \int_{-1}^1 \langle \vec{\mathbf{k}} | \mathbf{K} | \vec{\mathbf{p}} \rangle P_l(\hat{\mathbf{k}} \cdot \hat{\mathbf{p}}) d(\hat{\mathbf{k}} \cdot \hat{\mathbf{p}}) &= \frac{1}{2} \int_{-1}^1 \langle \vec{\mathbf{k}} | \mathbf{V} | \vec{\mathbf{p}} \rangle P_l(\hat{\mathbf{k}} \cdot \hat{\mathbf{p}}) d(\hat{\mathbf{k}} \cdot \hat{\mathbf{p}}) \\ &- \frac{1}{16\pi^3} \int_{-1}^1 d(\hat{\mathbf{k}} \cdot \hat{\mathbf{p}}) \int d^3q \langle \vec{\mathbf{k}} | \mathbf{V} | \vec{\mathbf{q}} \rangle \frac{m\Omega}{\hbar^2 q^2} \langle \vec{\mathbf{q}} | \mathbf{K} | \vec{\mathbf{p}} \rangle P_l(\hat{\mathbf{k}} \cdot \hat{\mathbf{p}}) \quad (\text{D2}) \end{aligned}$$

Let $\langle \vec{\mathbf{k}} | \mathbf{K} | \vec{\mathbf{p}} \rangle \equiv \sum_l (2l + 1) P_l(\hat{\mathbf{k}} \cdot \hat{\mathbf{p}}) \langle \mathbf{k} | \mathbf{K} | \mathbf{p} \rangle_l$ and $\langle \vec{\mathbf{k}} | \mathbf{V} | \vec{\mathbf{p}} \rangle \equiv \sum_l (2l + 1) P_l(\hat{\mathbf{k}} \cdot \hat{\mathbf{p}}) \langle \mathbf{k} | \mathbf{V} | \mathbf{p} \rangle_l$;

then $\langle \mathbf{k} | \mathbf{K} | \mathbf{p} \rangle_l = \frac{1}{2} \int_{-1}^1 \langle \vec{\mathbf{k}} | \mathbf{K} | \vec{\mathbf{p}} \rangle P_l(\hat{\mathbf{k}} \cdot \hat{\mathbf{p}}) d(\hat{\mathbf{k}} \cdot \hat{\mathbf{p}})$ and

$\langle \mathbf{k} | \mathbf{V} | \mathbf{p} \rangle_l = \frac{1}{2} \int_{-1}^1 \langle \vec{\mathbf{k}} | \mathbf{V} | \vec{\mathbf{p}} \rangle P_l(\hat{\mathbf{k}} \cdot \hat{\mathbf{p}}) d(\hat{\mathbf{k}} \cdot \hat{\mathbf{p}})$.

Equation (D2) reads, with several substitutions, as follows:

$$\begin{aligned}
\langle \mathbf{k} | \mathbf{K} | \mathbf{p} \rangle_{\ell} &= \langle \mathbf{k} | \mathbf{V} | \mathbf{p} \rangle_{\ell} - \frac{1}{16\pi^3} \int_{-1}^1 d(\hat{\mathbf{k}} \cdot \hat{\mathbf{p}}) \int_0^{\infty} q^2 dq \int_0^{2\pi} d\varphi \int_{-1}^1 d(\hat{\mathbf{k}} \cdot \hat{\mathbf{q}}) \\
&\times \sum_{\ell'} (2\ell' + 1) P_{\ell', (\hat{\mathbf{k}} \cdot \hat{\mathbf{q}})} \langle \mathbf{k} | \mathbf{V} | \mathbf{q} \rangle_{\ell'} \frac{m\Omega}{\hbar^2 q^2} \\
&\times \sum_{\ell''} (2\ell'' + 1) P_{\ell'', (\hat{\mathbf{q}} \cdot \hat{\mathbf{p}})} \langle \mathbf{q} | \mathbf{K} | \mathbf{p} \rangle_{\ell''} P_{\ell}(\hat{\mathbf{k}} \cdot \hat{\mathbf{p}}) \quad (\text{D3})
\end{aligned}$$

where φ is the azimuthal angle of \mathbf{q} . Figure 15 shows angular variables which are related to $\hat{\mathbf{k}}$, $\hat{\mathbf{p}}$, and $\hat{\mathbf{q}}$ by $\cos \theta_0 = \hat{\mathbf{k}} \cdot \hat{\mathbf{p}}$, $\cos \omega = \hat{\mathbf{k}} \cdot \hat{\mathbf{q}}$, and $\cos \nu = \hat{\mathbf{p}} \cdot \hat{\mathbf{q}}$. The variable ν can be eliminated by using the addition formula for spherical harmonics (see, for example, Morse and Feshbach (ref. 43))

$$P_{\ell'', (\cos \nu)} = \sum_{m=0}^{\ell''} \epsilon_m \frac{(\ell'' - m)!}{(\ell'' + m)!} P_{\ell'', (\cos \theta_0)}^m P_{\ell'', (\cos \omega)}^m \cos(m\varphi) \quad \epsilon_0 = 1, \epsilon_m = 2, m > 1$$

or

$$P_{\ell'', (\hat{\mathbf{p}} \cdot \hat{\mathbf{q}})} = \sum_{m=0}^{\ell''} \epsilon_m \frac{(\ell'' - m)!}{(\ell'' + m)!} P_{\ell'', (\hat{\mathbf{k}} \cdot \hat{\mathbf{p}})}^m P_{\ell'', (\hat{\mathbf{k}} \cdot \hat{\mathbf{q}})}^m \cos(m\varphi) \quad (\text{D4})$$

But in integrating equation (D3) over φ , only the $m = 0$ term of equation (D4) will survive, so equation (D3) becomes, substituting for $P_{\ell}(\hat{\mathbf{p}} \cdot \hat{\mathbf{q}})$,

$$\begin{aligned}
\langle \mathbf{k} | \mathbf{K} | \mathbf{p} \rangle_l &= \langle \mathbf{k} | \mathbf{V} | \mathbf{p} \rangle_l - \frac{1}{8\pi^2} \int_{-1}^1 d(\hat{\mathbf{k}} \cdot \hat{\mathbf{p}}) \int_0^\infty dq \int_{-1}^1 d(\hat{\mathbf{k}} \cdot \hat{\mathbf{q}}) \sum_{l', l''} (2l' + 1)(2l'' + 1) \\
&\quad \times \langle \mathbf{k} | \mathbf{V} | \mathbf{q} \rangle_{l'} \frac{m\Omega}{\hbar^2} \langle \mathbf{q} | \mathbf{K} | \mathbf{p} \rangle_{l''} P_{l'}(\hat{\mathbf{k}} \cdot \hat{\mathbf{q}}) P_{l''}(\hat{\mathbf{k}} \cdot \hat{\mathbf{q}}) P_l(\hat{\mathbf{k}} \cdot \hat{\mathbf{p}}) \\
&= \langle \mathbf{k} | \mathbf{V} | \mathbf{p} \rangle_l - \frac{1}{8\pi^2} \int_{-1}^1 d(\hat{\mathbf{k}} \cdot \hat{\mathbf{p}}) \int_0^\infty dq \sum_{l'} 2(2l' + 1) \langle \mathbf{k} | \mathbf{V} | \mathbf{q} \rangle_{l'} \frac{m\Omega}{\hbar^2} \\
&\quad \times \langle \mathbf{q} | \mathbf{K} | \mathbf{p} \rangle_{l'} P_{l'}(\hat{\mathbf{k}} \cdot \hat{\mathbf{p}}) P_l(\hat{\mathbf{k}} \cdot \hat{\mathbf{p}})
\end{aligned}$$

or

$$\langle \mathbf{k} | \mathbf{K} | \mathbf{p} \rangle_l = \langle \mathbf{k} | \mathbf{V} | \mathbf{p} \rangle_l - \frac{1}{2\pi^2} \int_0^\infty dq \langle \mathbf{k} | \mathbf{V} | \mathbf{q} \rangle_l \frac{m\Omega}{\hbar^2} \langle \mathbf{q} | \mathbf{K} | \mathbf{p} \rangle_l \quad (\text{D5a})$$

This last equation may be solved for any l , and the entire reaction matrix may then be found by

$$\langle \vec{\mathbf{k}} | \mathbf{K} | \vec{\mathbf{p}} \rangle = \sum_l (2l + 1) P_l(\hat{\mathbf{k}} \cdot \hat{\mathbf{p}}) \langle \mathbf{k} | \mathbf{K} | \mathbf{p} \rangle_l \quad (\text{D5b})$$

The calculations by machine are simpler when the equations are written in dimensionless form, and the resulting forms are those required in equation (13). Recall that

$$\mathcal{K} \equiv \frac{\Omega}{4\pi} \frac{m}{\hbar^2 a} \mathbf{K} \quad \text{and} \quad \mathcal{V} \equiv \frac{ma^2}{\hbar^2} \mathbf{V}. \quad \text{Multiplying equation (D5a) by } \frac{\Omega}{4\pi} \frac{m}{\hbar^2 a} \text{ gives}$$

$$\langle \mathbf{k} | \frac{\Omega m}{4\pi \hbar^2 a} \mathbf{K} | \mathbf{p} \rangle_l = \frac{1}{4\pi} \langle \mathbf{k} | \frac{\Omega m}{\hbar^2 a} \mathbf{V} | \mathbf{p} \rangle_l - \frac{1}{2\pi^2} \int_0^\infty d(qa) \langle \mathbf{k} | \frac{\Omega m}{\hbar^2 a} \mathbf{V} | \mathbf{q} \rangle_l \langle \mathbf{q} | \frac{\Omega m}{4\pi \hbar^2 a} \mathbf{K} | \mathbf{p} \rangle_l$$

Note that

$$\begin{aligned}
\langle \mathbf{k} | \frac{\Omega m}{\hbar^2 a} \mathbf{K} | \mathbf{p} \rangle_l &= \frac{1}{2} \int_{-1}^1 d(\hat{\mathbf{k}} \cdot \hat{\mathbf{p}}) P_l(\hat{\mathbf{k}} \cdot \hat{\mathbf{p}}) \frac{\Omega m}{\hbar^2 a} \int d^3 r \langle \bar{\mathbf{k}} | \bar{\mathbf{r}} \rangle V(\mathbf{r}) \langle \bar{\mathbf{r}} | \bar{\mathbf{p}} \rangle \\
&= \frac{1}{2\Omega} \int_{-1}^1 d(\hat{\mathbf{k}} \cdot \hat{\mathbf{p}}) P_l(\hat{\mathbf{k}} \cdot \hat{\mathbf{p}}) \frac{\Omega m}{\hbar^2 a} \int_0^\infty r^2 dr V(r) \int_{-1}^1 d(\hat{\mathbf{k}} \cdot \hat{\mathbf{r}}) \sum_{l', l''} (2l' + 1) \\
&\quad \times (2l'' + 1) P_{l'}(\hat{\mathbf{k}} \cdot \hat{\mathbf{r}}) P_{l''}(\hat{\mathbf{p}} \cdot \hat{\mathbf{r}}) i^{l' - l''} j_{l'}(kr) j_{l''}(pr) \int_0^{2\pi} d\varphi
\end{aligned}$$

and

$$\langle \bar{\mathbf{k}} | \bar{\mathbf{r}} \rangle = \sum_l i^l (2l + 1) P_l(\hat{\mathbf{k}} \cdot \hat{\mathbf{r}})$$

Then

$$\begin{aligned}
\langle \mathbf{k} | \frac{\Omega m}{\hbar^2 a} V | \mathbf{p} \rangle_l &= 2\pi \int_{-1}^1 d(\hat{\mathbf{k}} \cdot \hat{\mathbf{p}}) P_l(\hat{\mathbf{k}} \cdot \hat{\mathbf{p}}) \frac{m}{\hbar^2 a} \int r^2 dr \sum_{l'} (2l' + 1) P_{l'}(\hat{\mathbf{p}} \cdot \hat{\mathbf{k}}) j_{l'}(kr) j_{l'}(pr) v(r) \\
&= 4\pi \frac{m}{\hbar^2 a} \int_0^\infty r^2 dr v(r) j_l(kr) j_l(pr) \\
&= 4\pi \int_0^\infty \gamma^2 j_l(ka\gamma) j_l(pa\gamma) \mathcal{V}(\gamma) d\gamma, \quad \gamma \equiv \frac{\mathbf{r}}{a}
\end{aligned}$$

where $j_l(x)$ is the spherical Bessel function of the first kind of order l . So

$$\langle k|\mathcal{X}|p\rangle_l = \langle k|\mathcal{V}|p\rangle_l - \frac{2}{\pi} \int_0^\infty d(qa) \langle k|\mathcal{V}|q\rangle_l \langle q|\mathcal{X}|p\rangle_l \quad (D6)$$

where

$$\langle k|\mathcal{V}|q\rangle_l \equiv \int_0^\infty \gamma^2 \mathcal{V}(\gamma) j_l(ka\gamma) j_l(qa\gamma) d\gamma \quad (D7)$$

Equation (D5a) or the dimensionless versions (eqs. (D6) and (D7)) can be solved rather simply with a computer for any potential for which $\langle k|V|p\rangle$ exists. The simplest method of solution is "guess and iterate." The partial wave components $\langle k|\mathcal{V}|p\rangle_l$ are first calculated in the dimensionless form (eq. (D7)), and then they are substituted into the right-hand side of equation (D6) along with the first guess for $\langle k|\mathcal{X}|p\rangle_l$. The resulting left-hand side could serve as the next approximation to $\langle k|\mathcal{X}|p\rangle_l$, but averaging that value with the original guess before starting a new iteration helps reduce or prevent "oscillations" about the final answer. The situation is rather analogous to underdamping, overdamping, or critical damping in a mechanical oscillator. The relative weighting of the old and new values of the elements $\langle k|\mathcal{X}|p\rangle_l$ determine the damping characteristics. Where the elements $\langle k|\mathcal{V}|p\rangle_l$ are large and the initial guesses for $\langle k|\mathcal{X}|p\rangle_l$ were not very close, a large relative weight had to be given to the n^{th} approximation in comparison to the $(n+1)^{\text{th}}$ in order to prevent overshooting the correct answer and oscillating about it.

For a hard core or any singular repulsive core that increases faster than $1/r$, $\langle k|\mathcal{V}|p\rangle_0$ (S-wave) does not exist, and higher partial waves may also be divergent. However, $\langle k|\mathcal{X}|p\rangle_l$ does exist for such potentials for any l if it is considered to be the limit of the class of solutions of equation (D5a) as a finite repulsive core is made progressively stronger. In fact, this is the way the integral equation was solved by machine. A modestly strong repulsive core was introduced for the first iteration, and the strength was increased each iteration until further increases had negligible effect on the resulting reaction matrix elements. Figure 16 shows the Y. S. potential with the core cut off at $V = 300$ and 400 . These energies correspond to $V/k = 684$ and 912 K. Values of the diagonal elements, $\langle p|\mathcal{X}|p\rangle_0$ (the S-wave component), of the reaction matrix differed by less than 1 percent for these two cutoffs. Further increase of the cutoff would have a still smaller effect on the elements. The higher partial waves are less sensitive to the core details because of the angular momentum barrier.

The matrix elements of V and K are square arrays of numbers. Storing these arrays for small enough increments between values and large enough ranges for good accuracy and doing the required numerical operations in a reasonable time on the computer was a real problem. For a given potential (such as Y. S.), about 5 minutes of computing

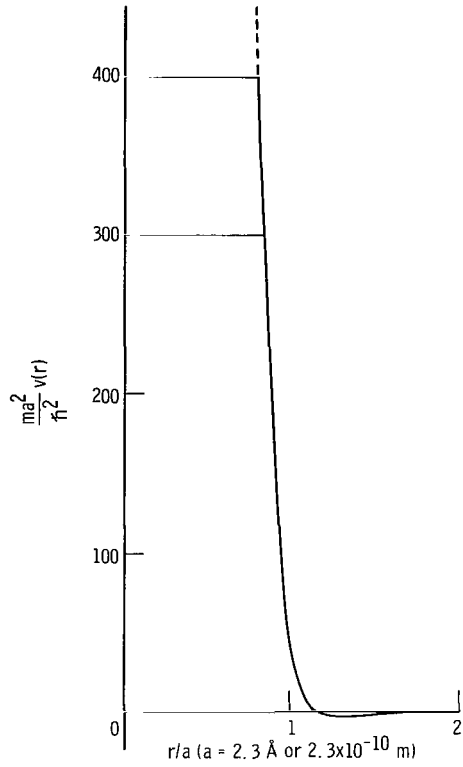


Figure 16. - Core cutoff of helium potential.

time was needed to calculate the \mathbf{K} matrix. Probably a more efficient method exists for solving the linear integral equation for \mathbf{K} , although the iterative method is undoubtedly the most straightforward.

From $\langle \vec{k} | \mathbf{K} | \vec{p} \rangle = \sum_l (2l + 1) P_l(\hat{k} \cdot \hat{p}) \langle k | \mathbf{K} | p \rangle_l$ it is evident that, if $\langle \vec{k} | \mathbf{K} | \vec{p} \rangle + \langle k | \mathbf{K} | -p \rangle$ occurs, the odd partial wave terms will cancel out because $\langle k | \mathbf{K} | p \rangle_l$ depends only on the magnitude of \vec{k} and \vec{p} whereas $P_l(\hat{k} \cdot \hat{p}) = \pm P_l(-\hat{k} \cdot \hat{p})$, depending on whether l is even (upper sign) or odd (lower sign). If either \vec{k} or \vec{p} is zero, then $\langle k | \mathbf{K} | p \rangle_l = 0$ for $l \neq 0$, so only the S-wave need be calculated.

APPENDIX E

BOGOLIUBOV TRANSFORMATION

The thermodynamically equivalent Hamiltonian is easily diagonalized by a Bogoliubov transformation. The form to be diagonalized is

$$H_{\text{TE}} = U + \sum_{\mathbf{k}} \left[f_{\mathbf{k}} a_{\mathbf{k}}^{\dagger} a_{\mathbf{k}} + \frac{1}{2} h_{\mathbf{k}} (a_{\mathbf{k}}^{\dagger} a_{-\mathbf{k}}^{\dagger} + a_{-\mathbf{k}} a_{\mathbf{k}}) \right]$$

This can be put into the form $H = U' + \sum_{\mathbf{k}} \epsilon_{\mathbf{k}} \alpha_{\mathbf{k}}^{\dagger} \alpha_{\mathbf{k}}$, where U' contains no operators, by making the following transformations:

$$a_{\mathbf{k}} \equiv u_{\mathbf{k}} \alpha_{\mathbf{k}} + v_{\mathbf{k}} \alpha_{-\mathbf{k}}^{\dagger}$$

and

$$a_{\mathbf{k}}^{\dagger} \equiv u_{\mathbf{k}} \alpha_{\mathbf{k}}^{\dagger} + v_{\mathbf{k}} \alpha_{-\mathbf{k}}$$

where $u_{\mathbf{k}} = u_{-\mathbf{k}} = u_{\mathbf{k}}^*$ and $v_{\mathbf{k}} = v_{-\mathbf{k}} = v_{\mathbf{k}}^*$. The transformation is canonical; that is, the new operators obey the same commutation rules as the old, if $u_{\mathbf{k}}^2 - v_{\mathbf{k}}^2 = 1$ for all \mathbf{k} . The transformation brings H_{TE} to the form

$$H_{\text{TE}} = U + \sum_{\mathbf{k}} \left\{ f_{\mathbf{k}} (u_{\mathbf{k}}^2 \alpha_{\mathbf{k}}^{\dagger} \alpha_{\mathbf{k}} + v_{\mathbf{k}}^2 \alpha_{-\mathbf{k}} \alpha_{-\mathbf{k}}^{\dagger}) + h_{\mathbf{k}} u_{\mathbf{k}} v_{\mathbf{k}} (\alpha_{\mathbf{k}}^{\dagger} \alpha_{\mathbf{k}} + \alpha_{-\mathbf{k}} \alpha_{-\mathbf{k}}^{\dagger}) \right. \\ \left. + \left[f_{\mathbf{k}} u_{\mathbf{k}} v_{\mathbf{k}} + \frac{1}{2} h_{\mathbf{k}} (u_{\mathbf{k}}^2 + v_{\mathbf{k}}^2) \right] (\alpha_{\mathbf{k}}^{\dagger} \alpha_{-\mathbf{k}}^{\dagger} + \alpha_{-\mathbf{k}} \alpha_{\mathbf{k}}) \right\}$$

This form explicitly shows the division of the Hamiltonian into diagonal and off-diagonal parts. The nondiagonal parts may be eliminated by the following choice for the remaining condition on $u_{\mathbf{k}}$ and $v_{\mathbf{k}}$:

$$f_{\mathbf{k}} u_{\mathbf{k}} v_{\mathbf{k}} + \frac{1}{2} h_{\mathbf{k}} (u_{\mathbf{k}}^2 + v_{\mathbf{k}}^2) = 0$$

for all k . By solving the two conditions on u_k and v_k , they can be eliminated from H_{TE} in favor of f_k , h_k , and ϵ_k . Then

$$u_k^2 = \frac{1}{2} \frac{f_k}{\epsilon_k} + 1$$

$$v_k^2 = \frac{1}{2} \frac{f_k}{\epsilon_k} - 1$$

and

$$u_k v_k = -\frac{h_k}{2\epsilon_k}$$

with $\epsilon_k = \sqrt{f_k^2 - h_k^2}$. The final result is

$$H_{\text{TE}} = U + \frac{1}{2} \sum_k (\epsilon_k - f_k) + \sum_k \epsilon_k \alpha_k^+ \alpha_k$$

If $\epsilon_k = 0$, the transformation is invalid.

Expressions for ξ_k and η_k can now be found. Luban shows (ref. 15) that the thermodynamic equivalence of H_{TE} with H_p holds if $\xi = \langle a_k^+ a_k \rangle$ and $\eta = \langle a_{-k} a_k^+ \rangle$, where averages are with respect to a grand ensemble. The set of states created by the α_k^+ are used to compute $\langle a_k^+ a_k \rangle$. These operators create noninteracting quasiparticles, and they obey Bose-Einstein commutation relations. Then

$$\begin{aligned} \langle a_k^+ a_k \rangle &= u_k^2 \langle \alpha_k^+ \alpha_k \rangle + v_k^2 \langle \alpha_{-k} \alpha_{-k}^+ \rangle + u_k v_k \langle \alpha_k^+ \alpha_{-k}^+ + \alpha_{-k} \alpha_k \rangle \\ &= u_k^2 \langle \alpha_k^+ \alpha_k \rangle + v_k^2 \langle 1 + \alpha_{-k}^+ \alpha_{-k} \rangle \\ &= (u_k^2 + v_k^2) \langle \alpha_k^+ \alpha_k \rangle + v_k^2 \end{aligned}$$

Using u_k^2 and v_k^2 from previous equations and noting the usual Bose occupation formula (for energy ϵ_k measured with respect to the chemical potential) result in

$$\begin{aligned}
\langle a_k^+ a_k \rangle &= \frac{f_k}{\epsilon_k} \frac{1}{e^{\beta \epsilon_k} - 1} + \frac{1}{2} \left(\frac{f_k}{\epsilon_k} - 1 \right) \\
&= \frac{1}{2} \left(\frac{f_k}{\epsilon_k} \frac{e^{\beta \epsilon_k} + 1}{e^{\beta \epsilon_k} - 1} - 1 \right) \\
&= \frac{1}{2} \left[\frac{f_k}{\epsilon_k} \coth \left(\frac{\beta \epsilon_k}{2} \right) - 1 \right]
\end{aligned}$$

and $\langle a_{-k} a_k \rangle$ is evaluated in similar fashion

$$\begin{aligned}
a_{-k} a_k &= (u_k \alpha_{-k} + v_k \alpha_k^+) (u_k \alpha_k + v_k \alpha_{-k}^+) \\
&= u_k^2 \alpha_{-k} \alpha_k + v_k^2 \alpha_k^+ \alpha_{-k}^+ + u_k v_k (\alpha_{-k} \alpha_{-k}^+ + \alpha_k^+ \alpha_k) \\
\langle a_{-k} a_k \rangle &= u_k v_k \langle \alpha_{-k} \alpha_{-k}^+ + \alpha_k^+ \alpha_k \rangle \\
&= u_k v_k \langle 2 \alpha_k^+ \alpha_k + 1 \rangle \\
&= -\frac{1}{2} \sqrt{\frac{f_k^2}{\epsilon_k^2} - 1} \left(\frac{2}{e^{\beta \epsilon_k} - 1} - 1 \right) \\
&= -\frac{1}{2} \frac{h_k}{\epsilon_k} \coth \left(\frac{\beta \epsilon_k}{2} \right)
\end{aligned}$$

APPENDIX F

RELATION BETWEEN K_{00} AND SCATTERING LENGTH

It will be shown here that $a \times \mathcal{K}_{00}$ is equal to the scattering length. The one-body reaction matrix used in this work has been defined using a zero-energy propagator. A diagonal element of the reaction matrix thus satisfies⁸

$$\langle p|K|p\rangle = \langle p|V|p\rangle + \sum_k \langle p|V|k\rangle \frac{m}{-\hbar^2 k^2} \langle k|K|p\rangle$$

The more commonly used reaction matrix K' has a nonzero propagator, that is,

$$\langle p|K'|p\rangle = \langle p|V|p\rangle + \sum_k \langle p|V|k\rangle \frac{m}{\hbar^2(p^2 - k^2)} \langle k|K'|p\rangle$$

This reaction matrix K' has the property that

$$\langle p|K'|p\rangle = \langle p|V|\psi_p\rangle$$

where V is the central potential, and $|\psi_p\rangle$ is an exact state of momentum p in the presence of the potential, and which is asymptotic to a plane wave plus a standing radial wave. (See, for example, Thaler (ref. 44).) Thus,

$$\langle p|K'|p\rangle = \frac{1}{\Omega} \int d^3r \varphi_p(\vec{r}) V(r) \psi_p(\vec{r})$$

where $\varphi_p(\vec{r})$ is a plane-wave function, $\psi_p(\vec{r})$ is the exact wave function, and Ω is the volume of the box containing the particle. For the limit as $p \rightarrow 0$ only the $l = 0$ partial wave contributes. Thus

⁸Vector signs on momenta are suppressed.

$$\begin{aligned}
\lim_{p \rightarrow 0} \langle p | \mathbf{K}' | p \rangle &= \lim_{p \rightarrow 0} \frac{4\pi}{\Omega} \int r^2 dr \varphi_p^{(0)}(r) V(r) R_p^{(0)}(r) \\
&= -\frac{4\pi}{\Omega} \frac{\hbar^2}{m} \lim_{p \rightarrow 0} \left(\frac{1}{p} \tan \delta_0^{(p)} \right) \\
&= \frac{4\pi}{\Omega} \frac{\hbar^2}{m} L
\end{aligned}$$

where $R_p^{(0)}(r)$ is the S-wave radial wave function, $\varphi_p^{(0)}(r)$ is the S-wave radial wave function of a plane wave, $L \equiv \lim_{p \rightarrow \infty} \left[\frac{1}{p} \tan \delta_0^{(p)} \right]$ is the scattering length, and $\delta_0^{(p)}$ is the S-wave phase shift for momentum p . Now, the diagonal element of \mathbf{K}' , $\langle p | \mathbf{K}' | p \rangle$, is continuous at $p = 0$; so

$$\langle 0 | \mathbf{K}' | 0 \rangle = \frac{4\pi}{\Omega} \frac{\hbar^2}{m} L$$

From the defining equations for \mathbf{K} and \mathbf{K}' , the elements $\langle 0 | \mathbf{K} | 0 \rangle$ and $\langle 0 | \mathbf{K}' | 0 \rangle$ can be expanded as follows:

$$\langle 0 | \mathbf{K} | 0 \rangle = \langle 0 | \mathbf{V} | 0 \rangle + \sum_{\mathbf{k}} \langle 0 | \mathbf{V} | \mathbf{k} \rangle \frac{m}{-\hbar^2 k^2} \langle \mathbf{k} | \mathbf{V} | 0 \rangle + \dots$$

and

$$\langle 0 | \mathbf{K}' | 0 \rangle = \langle 0 | \mathbf{V} | 0 \rangle + \sum_{\mathbf{k}} \langle 0 | \mathbf{V} | \mathbf{k} \rangle \frac{m}{-\hbar^2 k^2} \langle \mathbf{k} | \mathbf{V} | 0 \rangle + \dots$$

Thus $\langle 0 | \mathbf{K} | 0 \rangle = \langle 0 | \mathbf{K}' | 0 \rangle$. Then

$$\begin{aligned}
\langle 0 | \mathcal{X} | 0 \rangle &= \frac{\Omega}{4\pi} \frac{m}{\hbar^2 a} \langle 0 | \mathbf{K} | 0 \rangle \\
&= \frac{1}{a} \frac{\Omega}{4\pi} \frac{m}{\hbar^2} \langle 0 | \mathbf{K}' | 0 \rangle \\
&= \frac{\mathbf{L}}{a}
\end{aligned}$$

Hence,

$$a \times \mathcal{X}_{00} \equiv a \langle 0 | \mathcal{X} | 0 \rangle = \mathbf{L}$$

APPENDIX G

APPROXIMATE EVALUATION OF SINANAGLU EFFECTIVE TWO-PARTICLE POTENTIAL

Only two-particle interactions have been included in this work. Sinanaglu (ref. 39) has given an approximate way to modify the two-particle potential $V(r)$ to include the influence of the other particles in the liquid. He finds that the attractive well of the interparticle potential may be weakened as much as 10 to 40 percent by the medium. The largest effects occur for different solvent and solute species. But for two atoms of the same element in the liquid of that element, he derives an effective potential of interaction between two atoms as

$$V^{\text{eff}}(r) = V_{\text{vacuum}}(r) \times B(r)$$

where to sufficient accuracy for helium:

$$B(r) = 1 - \frac{\frac{1}{4}(n_1^2 - 1)L(r, \sigma)}{(n_1^2 + 2) \left[1 - \left(\frac{\sigma}{r}\right)^6 \right]}$$

where n_1 is the zero-frequency index of refraction, σ is the position of the zero of $V(r)$ if the vacuum potential is represented by the Lennard-Jones 6-12 potential. The function $L(r, \sigma)$ is given graphically (ref. 39) from numerical calculations. It is essentially equal to 2 for $(r/\sigma) \gtrsim 3$. For $1.6 < (r/\sigma) < 3$, $L(r, \sigma) \approx \frac{2}{3} \left(\frac{r}{\sigma} - 1.3 \right)$; for $0.5 < (r/\sigma) < 1.6$, $L(r, \sigma) \approx 0.3[(r/\sigma) - 0.5]^2$; and for $(r/\sigma) < 0.5$, $L(r, \sigma) = 0$. For values taken directly from the graph of reference 39 for L , the function $B(r)$ differs from one by about 1 percent at the most. The main reason there is such a small reduction of strength for helium (compared with an order of magnitude more in some other liquids considered by Sinanaglu) is that n_1 , the index of refraction, is only 1.03 for helium whereas for many liquids it is 1.3 or 1.4. Thus $n_1 - 1$ is only one-tenth as large for helium as for many liquids.

APPENDIX H

THE THIRD SEMIINVARIANT

The third semiinvariant M_3 has been defined as

$$M_3 = \frac{1}{\beta} \int_0^\beta d\lambda \int_0^\lambda d\lambda' \int_0^{\lambda'} d\lambda'' [\langle H'(\lambda)H'(\lambda')H'(\lambda'') \rangle - 3\langle H'(\lambda)H'(\lambda') \rangle \langle H'(\lambda'') \rangle + 2\langle H'(\lambda) \rangle \langle H'(\lambda') \rangle \langle H'(\lambda'') \rangle]$$

where

$$H' = \frac{1}{2} \sum_{k_1 k_2 k_3 k_4} \langle k_1 k_2 | V | k_3 k_4 \rangle a_{k_1}^+ a_{k_2}^+ a_{k_3} a_{k_4}$$

and

$$H'(\lambda) = \frac{1}{2} \sum_{k_1 k_2 k_3 k_4} \langle k_1 k_2 | V | k_3 k_4 \rangle e^{\lambda(\omega_{k_1} + \omega_{k_2} - \omega_{k_3} - \omega_{k_4})} a_{k_1}^+ a_{k_2}^+ a_{k_3} a_{k_4}$$

Only contributions from the $\langle H'(\lambda)H'(\lambda')H'(\lambda'') \rangle$ term will survive cancellation; so consider only that term, which will be denoted by M_3' ,

$$\begin{aligned}
M_3 &\equiv \frac{1}{\beta} \int_0^\beta d\lambda \int_0^\lambda d\lambda' \int_0^{\lambda'} d\lambda'' \langle H'(\lambda) H'(\lambda') H'(\lambda'') \rangle \\
&\xrightarrow{\beta \rightarrow \infty} \frac{1}{2} \sum_{\substack{k_1, k_2 \neq 0 \\ k_1 \neq k_2}} \frac{1}{\beta} \int_0^\beta d\lambda \int_0^\lambda d\lambda' \int_0^{\lambda'} d\lambda'' \langle 00 | V | k_1 - k_1 \rangle \\
&\quad \times \langle k_1 - k_1 | V | k_2 - k_2 \rangle \langle k_2 - k_2 | V | 00 \rangle e^{(\hbar^2/m) \left[-2\lambda k_1^2 + 2\lambda' (k_1^2 - k_2^2) + 2\lambda'' k_2^2 \right]} \\
&\quad \times \langle 0 | a_0^\dagger a_0^\dagger a_{k_1} a_{-k_1} a_{k_1}^\dagger a_{-k_1}^\dagger a_{k_2} a_{-k_2} a_{k_2}^\dagger a_{-k_2}^\dagger a_0 a_0 | 0 \rangle \\
&\quad + \frac{1}{2} \sum_{k \neq 0} \frac{1}{\beta} \int_0^\beta d\lambda \int_0^\lambda d\lambda' \int_0^{\lambda'} d\lambda'' \langle 00 | V | k - k \rangle \langle k 0 | V | k 0 \rangle \langle k - k | V | 00 \rangle \\
&\quad \times e^{(\hbar^2/m) (-2\lambda k^2 + 2\lambda'' k^2)} \langle 0 | a_0^\dagger a_0^\dagger a_k a_{-k} a_k^\dagger a_{-k}^\dagger a_0 a_0 a_k^\dagger a_{-k}^\dagger a_0 a_0 | 0 \rangle \\
&\quad + \text{terms that cancel with other parts of the semiinvariant}
\end{aligned}$$

From this point pursue only the terms that do not cancel. These terms become

$$\begin{aligned}
&\frac{1}{2} \sum_{\substack{k_1, k_2 \neq 0 \\ k_1 \neq k_2}} \frac{1}{\beta} \int_0^\beta d\lambda \int_0^\lambda d\lambda' \int_0^{\lambda'} d\lambda'' \frac{\hat{v}(k_1)}{\Omega} \frac{\hat{v}(k_1 - k_2)}{\Omega} \frac{\hat{v}(k_2)}{\Omega} e^{(\hbar^2/m) \left[-2\lambda k_1^2 + 2\lambda' (k_1^2 - k_2^2) + 2\lambda'' k_2^2 \right]} N^2 \\
&\quad + \frac{1}{2} \sum_{k \neq 0} \frac{1}{\beta} \int_0^\beta d\lambda \int_0^\lambda d\lambda' \int_0^{\lambda'} d\lambda'' \frac{\hat{v}(k)}{\Omega} \frac{\hat{v}(0)}{\Omega} \frac{\hat{v}(k)}{\Omega} e^{(\hbar^2/m) (-2\lambda k^2 + 2\lambda'' k^2)} N^3
\end{aligned}$$

where terms proportional to powers of N less than one have been dropped and it has been recognized that $\langle 0 | a_k^\dagger a_k | 0 \rangle = 0$ for $k \neq 0$. Further manipulation yields

$$\begin{aligned}
& \frac{1}{2} \frac{\rho N}{\beta \Omega^2} \sum_{\substack{k_1, k_2 \neq 0 \\ k_1 \neq k_2}} \hat{v}(k_1) \hat{v}(k_1 - k_2) \hat{v}(k_2) \int_0^\beta d\lambda \int_0^\lambda d\lambda' e^{(\hbar^2/m) \left[-2\lambda k_1^2 + 2\lambda' (k_1^2 - k_2^2) \right]} e^{\frac{(\hbar^2/m) 2\lambda' k_2^2 - 1}{2\hbar^2 k_2^2} - 1} \\
& + \frac{1}{2} \frac{\rho^2 N}{\beta \Omega} \sum_{k \neq 0} \hat{v}^2(k) \hat{v}(0) \int_0^\beta d\lambda \int_0^\lambda d\lambda' e^{-(\hbar^2/m) 2\lambda k^2} e^{\frac{(\hbar^2/m) 2\lambda' k^2 - 1}{2\hbar^2 k^2} - 1} \\
& = \frac{1}{2} \frac{\rho N}{\beta \Omega^2} \sum_{\substack{k_1, k_2 \neq 0 \\ k_1 \neq k_2}} \frac{m^2}{\hbar^4} \hat{v}(k_1) \hat{v}(k_1 - k_2) \frac{\hat{v}(k_2)}{2k_2^2} \int_0^\beta d\lambda e^{-(\hbar^2/m) 2\lambda k_1^2} \left[e^{\frac{(\hbar^2/m) 2\lambda k_1^2 - 1}{2k_1^2} - 1} - e^{\frac{(\hbar^2/m) 2(k_1^2 - k_2^2) - 1}{2(k_1^2 - k_2^2)} - 1} \right] \\
& + \frac{1}{2} \frac{\rho^2 N}{\beta \Omega} \sum_{k \neq 0} \frac{m}{\hbar^2} \frac{\hat{v}^2(k)}{2k^2} \hat{v}(0) \left\{ \frac{\beta}{\frac{2\hbar^2 k^2}{m}} + \frac{e^{-(\hbar^2/m) 2\beta k^2} - 1}{\frac{4\hbar^4 k^4}{m^2}} + \left[\frac{e^{-(\hbar^2/m) 2\lambda k^2}}{4\hbar^2 k^2 / m^2} \left(\frac{2\lambda \hbar^2 k^2}{m} + 1 \right) \right]_0^\beta \right\} \\
& \xrightarrow{\beta \rightarrow \infty} \frac{1}{8} \left[\frac{\rho N}{\Omega^2} \frac{m^2}{\hbar^4} \sum_{\substack{k_1, k_2 \neq 0 \\ k_1 \neq k_2}} \frac{\hat{v}(k_1)}{k_1^2} \frac{\hat{v}(k_2)}{k_2^2} \hat{v}(k_1 - k_2) + \frac{1}{8} \frac{\rho^2 N}{\Omega} \frac{m^2}{\hbar^4} \hat{v}(0) \sum_{k \neq 0} \frac{v^2(k)}{k^4} \right]
\end{aligned}$$

Thus for $\beta \rightarrow \infty$

$$M_3 = \frac{\rho N}{8} \frac{1}{(2\pi)^6} \frac{m^2}{\hbar^4} \int d^3 k_1 \int d^3 k_2 \frac{\hat{v}(k_1)}{k_1^2} \frac{\hat{v}(k_2)}{k_2^2} \hat{v}(k_1 - k_2) + \frac{\rho^2 N}{8} \frac{1}{(2\pi)^3} \frac{m^2}{\hbar^4} \hat{v}(0) \int d^3 k \frac{\hat{v}^2(k)}{k^4}$$

REFERENCES

1. Landau, L. : The Theory of Superfluidity of Helium II. *J. Phys. USSR*, vol. 5, no. 1, 1941, pp. 71-90.
2. Landau, L. : On the Theory of Superfluidity of Helium II. *J. Phys. USSR*, vol. 11, no. 1, 1947, pp. 91-92.
3. Yarnell, J. L. ; Arnold, G. P. ; Bendt, P. J. ; and Kerr, E. C. : Excitations in Liquid Helium: Neutron Scattering Measurements. *Phys. Rev.*, vol. 113, no. 6, Mar. 15, 1959, pp. 1379-1386.
4. Palevsky, H. ; Otnes, K. ; Larsson, K. E. ; Pauli, R. ; and Stedman, R. : Excitation of Rotons in Helium II by Cold Neutrons. *Phys. Rev.*, vol. 108, no. 5, Dec. 1, 1957, pp. 1346-1347.
5. Palevsky, H. ; Otnes, K. ; and Larsson, K. E. : Excitation of Rotons in Helium II by Cold Neutrons. *Phys. Rev.*, vol. 112, no. 1, Oct. 1, 1958, pp. 11-18.
6. Feynman, R. P. : Atomic Theory of the Two-Fluid Model of Liquid Helium. *Phys. Rev.*, vol. 94, no. 2, Apr. 15, 1954, pp. 262-277.
7. Beaumont, C. F. A. ; and Reekie, J. : Atomic Distribution in Liquid Helium. *Proc. Roy. Soc., Ser. A.*, vol. 228, no. 1174, Mar. 8, 1955, pp. 363-376.
8. Cohen, Michael; and Feynman, Richard P. : Theory of Inelastic Scattering of Cold Neutrons from Liquid Helium. *Phys. Rev.*, vol. 107, no. 1, July 1, 1957, pp. 13-24.
9. Pines, David: *The Many-Body Problem*. W. A. Benjamin, Inc., 1961, p. 10.
10. Bogolubov, N. : On the Theory of Superfluidity. *J. Phys. USSR*, vol. 11, no. 1, 1947, pp. 23-32.
11. Bogoliubov, N. N. ; and Zubarev, D. N. : The Wave Function of the Lowest State of a System of Interacting Bose Particles. *Soviet Phys.-JETP*, vol. 1, no. 1, July 1955, pp. 83-90.
12. Brueckner, K. A. ; and Sawada, K. : Bose-Einstein Gas with Repulsive Interactions: General Theory. *Phys. Rev.*, vol. 106, no. 6, June 15, 1957, pp. 1117-1127.
13. Brueckner, K. A. ; and Sawada, K. : Bose-Einstein Gas with Repulsive Interactions: Hard Spheres at High Density. *Phys. Rev.*, vol. 106, no. 6, June 15, 1957, pp. 1128-1135.
14. Wentzel, G. : Thermodynamically Equivalent Hamiltonian for Some Many-Body Problems. *Phys. Rev.*, vol. 120, no. 5, Dec. 1, 1960, pp. 1572-1575.

15. Luban, Marshall: Statistical Mechanics of a Nonideal Boson Gas: Pair Hamiltonian Model. *Phys. Rev.*, vol. 128, no. 2, Oct. 15, 1962, pp. 965-987.
16. Foldy, Leslie L.: Charged Boson Gas. *Phys. Rev.*, vol. 124, no. 3, Nov. 1, 1961, pp. 649-651.
17. Parry, W. E.; and ter Haar, D.: On the Theory of Relaxation Processes in Liquid Helium. *Ann. Phys. (N.Y.)*, vol. 19, no. 3, Sept. 1962, pp. 496-539.
18. Abe, R.: Quantum-Mechanical Many-Body Problem with Hard-Sphere Interaction. *Progr. Theor. Phys.*, vol. 19, no. 6, June 1958, pp. 699-712.
19. Abe, R.: Quantum Mechanics of Strongly Interacting Particles with an Application to Lennard-Jones Potential. *Progr. Theor. Phys.*, vol. 19, no. 6, June 1958, pp. 713-724.
20. Liu, L.; Liu, Lu Sun; and Wong, K. W.: Hard-Sphere Approach to the Excitation Spectrum in Liquid Helium II. *Phys. Rev.*, vol. 135A, no. 5, Aug. 31, 1964, pp. 1166-1172.
21. Girardeau, M.; and Arnowitt, R.: Theory of Many-Boson Systems: Pair Theory. *Phys. Rev.*, vol. 113, no. 3, Feb. 1, 1959, pp. 755-761.
22. Girardeau, M.: Relationship Between Systems of Impenetrable Bosons and Fermions in One Dimension. *J. Math. Phys.*, vol. 1, no. 6, Nov.-Dec. 1960, pp. 516-523.
23. Girardeau, M.: Simple and Generalized Condensation in Many-Boson Systems. *Phys. Fluids*, vol. 5, no. 11, Nov. 1962, pp. 1468-1478.
24. Bardeen, J.; Cooper, L. N.; and Schrieffer, J. R.: Microscopic Theory of Superconductivity. *Phys. Rev.*, vol. 106, no. 1, Apr. 1, 1957, pp. 162-164.
25. Bardeen, J.; Cooper, L. N.; and Schrieffer, J. R.: Theory of Superconductivity. *Phys. Rev.*, vol. 108, no. 5, Dec. 1, 1957, pp. 1175-1204.
26. Yntema, J. L.; and Schneider, W. G.: Compressibility of Gases at High Temperatures. III. The Second Virial Coefficient of Helium in the Temperature Range of 600^o C to 1200^o C. *J. Chem. Phys.*, vol. 18, no. 5, May 1950, pp. 641-646.
27. Yntema, J. L.; and Schneider, W. G.: On the Intermolecular Potential of Helium. *J. Chem. Phys.*, vol. 18, no. 5, May 1950, pp. 646-650.
28. Sawada, K.; and Vasudevan, R.: Simplified Model of Liquid Helium. *Phys. Rev.*, vol. 124, no. 2, Oct. 15, 1961, pp. 300-307.
29. Slater, John C.; and Kirkwood, John G.: The van der Waals Forces in Gases. *Phys. Rev.*, vol. 37, no. 6, Mar. 15, 1931, pp. 682-697.

30. Slater, J. C. : The Normal State of Helium. *Phys. Rev.*, vol. 32, no. 3, Sept. 1928, pp. 349-360.
31. London, F. : Zur Theorie und Systematik der Molekularkräfte. *Z. Physik*, vol. 63, July 14, 1930, pp. 245-279.
32. Margenau, H. : Van der Waals Forces. *Rev. Mod. Phys.*, vol. 11, no. 1, Jan. 1939, pp. 1-35.
33. London, Fritz: Macroscopic Theory of Superfluid Helium. Vol. 2 of Superfluids. John Wiley & Sons, Inc., 1954, p. 21.
34. Brueckner, K. A. ; and Gammel, J. L. : Properties of Liquid He³ at Low Temperature. *Phys. Rev.*, vol. 109, no. 4, Feb. 15, 1958, pp. 1040-1046.
35. White, David; Rubin, Thor; Camky, Paul; and Johnston, H. L. : The Virial Coefficients of Helium from 20 to 300⁰ K. *J. Phys. Chem.*, vol. 64, no. 11, Nov. 1960, pp. 1607-1612.
36. Kilpatrick, John E. ; Keller, William E. ; Hammel, Edward F. ; and Metropolis, Nicholas: Second Virial Coefficients of He³ and He⁴. *Phys. Rev.*, vol. 94, no. 5, June 1, 1954, pp. 1103-1110.
37. deBoer, J. ; and Michels, A. : Quantum-Mechanical Calculation of the Second Virial-Coefficient of Helium at Low Temperatures. *Physica*, vol. 6, May 1939, pp. 409-420.
38. Dalgarno, A. ; and Victor, G. A. : Long Range Three-Body Forces Between Helium and Hydrogen Atoms. *Molecular Phys.*, vol. 10, no. 4, 1966, pp. 333-337.
39. Singanoglu, O. : Intermolecular Forces in Liquids. Center for Theoretical Studies, Univ. Miami, Florida, Feb. 1967.
40. Pitaevskii, L. P. : Attraction of Small Particles Suspended in a Liquid at Large Distances. *Soviet Phys.-JETP*, vol. 10, no. 2, Feb. 1960, pp. 408-409.
41. Brout, R. H. ; and Carruthers, P. : Lectures on the Many-Electron Problem. Interscience Publ., 1963.
42. Kubo, Ryogo: Generalized Cumulant Expansion Method. *J. Phys. Soc. Japan*, vol. 17, no. 7, July 1962, pp. 1100-1120.
43. Morse, Philip M. ; and Feshbach, Herman: Methods of Theoretical Physics. McGraw-Hill Book Co., Inc., 1953, p. 1274.
44. Thaler, R. M. : Introduction to the Theory of Scattering. Lectures in Theoretical Physics. Vol. 4, Wesley E. Brittin, W. B. Downs, and Joanne Downs, eds., Interscience Publ., 1963.

FIRST CLASS MAIL

05U 001 49 51 3DS 68285 00903
AIR FORCE WEAPONS LABORATORY/AFWL/
KIRTLAND AIR FORCE BASE, NEW MEXICO 8711

ATTN: F. LOU BOWMAN, ACTING CHIEF TECH. LIAISON

POSTMASTER: If Undeliverable (Section 1
Postal Manual) Do Not Return

"The aeronautical and space activities of the United States shall be conducted so as to contribute . . . to the expansion of human knowledge of phenomena in the atmosphere and space. The Administration shall provide for the widest practicable and appropriate dissemination of information concerning its activities and the results thereof."

— NATIONAL AERONAUTICS AND SPACE ACT OF 1958

NASA SCIENTIFIC AND TECHNICAL PUBLICATIONS

TECHNICAL REPORTS: Scientific and technical information considered important, complete, and a lasting contribution to existing knowledge.

TECHNICAL NOTES: Information less broad in scope but nevertheless of importance as a contribution to existing knowledge.

TECHNICAL MEMORANDUMS: Information receiving limited distribution because of preliminary data, security classification, or other reasons.

CONTRACTOR REPORTS: Scientific and technical information generated under a NASA contract or grant and considered an important contribution to existing knowledge.

TECHNICAL TRANSLATIONS: Information published in a foreign language considered to merit NASA distribution in English.

SPECIAL PUBLICATIONS: Information derived from or of value to NASA activities. Publications include conference proceedings, monographs, data compilations, handbooks, sourcebooks, and special bibliographies.

TECHNOLOGY UTILIZATION PUBLICATIONS: Information on technology used by NASA that may be of particular interest in commercial and other non-aerospace applications. Publications include Tech Briefs, Technology Utilization Reports and Notes, and Technology Surveys.

Details on the availability of these publications may be obtained from:

SCIENTIFIC AND TECHNICAL INFORMATION DIVISION
NATIONAL AERONAUTICS AND SPACE ADMINISTRATION
Washington, D.C. 20546